Challenges and opportunities offered by geostationary space observations for air quality research and emission monitoring

Tai-Long He,[⋆a,b] Glenn-Michael Oomen,[⋆c] Idir Bouarar,[d] Kelly Chance,[e] Cathy Clerbaux,[f,g] David P. Edwards,[h] Henk Eskes,[i] Benjamin Gaubert,[h] Claire Granier,[j,k,l] Marc Guevara,[m] Daniel J. Jacob,[b] Jennifer Kaiser,[n,o] Jhoon Kim,[p] Shobha Kondragunta,[q] Xiong Liu,[e] Kazuyuki Miyazaki,[r] Eloise A. Marais,[s] Rokjin Park,[t] Vincent-Henri Peuch,[u] Gabriele Pfister,[h] Andreas Richter,[v] Trissevgeni Stavrakou,[c] Wenfu Tang,[h] Raid M. Suleiman,[e] Alexander J. Turner,[a] Ben Veihelmann,[w] Zhao-Cheng Zeng,[x] Guy P. Brasseur,[d]

[⋆] *These authors contributed equally to this work.*

[a] *Department of Atmospheric Sciences, University of Washington, Seattle, Washington, USA*

[b] *John A. Paulson School of Engineering and Applied Sciences, Harvard University, Cambridge, 02138, USA*

[c] *Royal Belgian Institute for Space Aeronomy (BIRA-IASB), Brussels, Belgium*

[d] *Max Planck Institute for Meteorology, Hamburg, Germany*

[e] *Smithsonian Astrophysical Observatory (SAO), Center for Astrophysics — Harvard & Smithsonian, Cambridge, MA 02138, USA*

[f] *LATMOS/IPSL, Sorbonne Université, UVSQ, CNRS, Paris 75005, France*

[g] *Spectroscopy, Quantum Chemistry and Atmospheric Remote Sensing (SQUARES), Université libre de Bruxelles (ULB), Brussels 1050, Belgium*

[h] *Atmospheric Chemistry Observations & Modeling Laboratory, NSF National Center for Atmospheric Research (NSF NCAR), Boulder, Colorado, USA*

[i] *Royal Netherlands Meteorological Institute, De Bilt, the Netherlands*

[j] *Laboratoire d'Aérologie, Université de Toulouse, CNRS, UPS, Toulouse, France*

[k] *NOAA Chemical Sciences Laboratory, Boulder, Colorado, USA*

[l] *CIRES, University of Colorado Boulder, Boulder, Colorado, USA*

[m] *Barcelona Supercomputing Center, 08034 Barcelona, Spain*

[n] *School of Civil and Environmental Engineering, Georgia Institute of Technology, Atlanta, GA, USA*

[o] *School of Earth and Atmospheric Sciences, Georgia Institute of Technology, Atlanta, GA, USA*

[p] *Department of Atmospheric Sciences, Yonsei University, Seoul, South Korea*

[q] *NOAA/NESDIS, College Park, Maryland*

[r] *Jet Propulsion Laboratory/California Institute for Technology, Pasadena, California, USA*

[s] *Department of Geography, University College London, London, UK*

[t] *School of Earth and Environmental Sciences, Seoul National University, Seoul, South Korea*

[u] *European Centre for Medium-Range Weather Forecasts, Reading, UK*

[v] *Institute of Environmental Physics, University of Bremen, Bremen, Germany*

[w] *ESA-ESTEC, Noordwijk, the Netherlands*

[x] *School of Earth and Space Sciences, Peking University, Beijing, 100871, China*

Corresponding author: Tai-Long He, the@g.harvard.edu

Corresponding author: Glenn-Michael Oomen, glenn-michael.oomen@aeronomie.be

ABSTRACT: Space-borne remote sensing of atmospheric chemical constituents is crucial for monitoring and better understanding global and regional air quality. Since the 1990s, the continuous development of instruments onboard low-Earth orbit (LEO) satellites has led to major advances in air quality research by providing daily global measurements of atmospheric chemical species. The next generation of atmospheric composition satellites measures from the geostationary Earth orbit (GEO) with hourly temporal resolution, allowing the observation of diurnal variations of air pollutants. The first two instruments of the GEO constellation coordinated by the Committee on Earth Observation Satellites (CEOS), the Geostationary Environment Monitoring Spectrometer (GEMS) for Asia and the Tropospheric Emissions: Monitoring Pollution (TEMPO) for North America, were successfully launched in 2020 and 2023, respectively. The European component, Sentinel-4, is planned for launch in 2025. This work provides an overview of satellite missions for atmospheric composition monitoring and the state of the science in air quality research. We cover recent advances in retrieval algorithms, the modeling of emissions and atmospheric chemistry, data assimilation, and the application of machine learning based on satellite data. We discuss the challenges and opportunities in air quality research in the era of GEO satellites, and provide recommendations on research priorities for the near future.

SIGNIFICANCE STATEMENT: Space-borne measurements of the chemical composition of the atmosphere are crucial for understanding and forecasting air quality. With the next generation of atmospheric composition satellites measuring from the geostationary Earth orbit, air quality research has entered a new era. We provide an overview of the constellation of satellites for atmospheric composition monitoring and review the latest advances in satellite-driven air quality research. We identify the challenges and opportunities for a better exploitation of the wealth of satellite data from a geostationary perspective.

CAPSULE: The International Space Science Institute International Expert Team has reviewed recent advances and discussed challenges and opportunities in air quality research in the era of geostationary atmospheric composition satellites.

1. Introduction

Air pollution is one of the leading causes of global premature mortality and economic damages (Cohen et al. 2017; Dechezleprêtre et al. 2019). Space-borne remote sensing instruments have played a key role in monitoring atmospheric composition since the 1990s (Burrows et al. 1999; Bovensmann et al. 1999; Drummond and Mand 1996; Veefkind et al. 2006, 2012; Zoogman et al. 2017; Levelt et al. 2018; Kim et al. 2020, among others). Satellite observations have been used with sophisticated models to help develop policies to reduce emissions (e.g., Duncan et al. 2016; Jiang et al. 2018), improve our knowledge about air pollution (e.g., Fu et al. 2007; Silvern et al. 2019; Yang et al. 2023b), and better forecast air quality (e.g., Peuch et al. 2022; Eskes et al. 2024). Efficient reduction of air pollution often contributes to the reduction of co-emitted greenhouse gases (GHGs) and towards the mitigation of climate change (West et al. 2013; Miyazaki and Bowman 2023).

Efforts have been made to improve the observation of atmospheric composition from space over the past two decades. The TROPOspheric Monitoring Instrument (TROPOMI; 2017–present; Veefkind et al. 2012) is the first to provide daily global multi-constituent measurements at a sub-10 km spatial resolution (Veefkind et al. 2012), which helps to reveal detailed linkages between human activities and air quality (e.g., Riess et al. 2022; Martínez-Alonso et al. 2023; Zuo et al. 2023). The next generation of atmospheric composition monitoring satellites measures column abundances of trace gases from the geostationary Earth orbit (GEO). The first two GEO atmospheric composition satellites, GEMS (Geostationary Environment Monitoring Spectrometer; Kim et al. 2020) for Asia and TEMPO (Tropospheric Emissions: Monitoring of Pollution; Zoogman et al. 2017) for North America, were successfully launched in 2020 and 2023, respectively. The European component, Sentinel-4, is planned for launched in 2025 (Stark et al. 2013). Ongoing LEO missions have been proposed to sustain atmospheric composition observations outside the GEO domains.

The International Space Science Institute (ISSI) offers the platform to facilitate international collaboration on interdisciplinary research in space science. The ISSI International Expert Team 489 (Brasseur and Granier 2020) recently assessed advancements in the use of space-borne instruments to improve air quality characterization and forecasts. We summarize the discussion and conclusions from the ISSI Team 489 Workshop (2023) in this paper to provide an overview of the opportunities and challenges arising in the era of GEO atmospheric composition satellites. The recently launched and scheduled satellite instruments motivate us to review the state of air quality research based on satellite observations. We cover advances in the development of retrieval algorithms, modeling and forecasting of air quality, data assimilation, and machine learning applications. We conclude with recommendations for research priorities for the near future to better exploit GEO satellite atmospheric composition observations.

2. Constellation of LEO and GEO atmospheric composition satellites

a. Heritage of LEO satellites

Column concentrations of short-lived air pollutants, including tropospheric ozone (O_3), nitrogen dioxide (NO_2), sulfur dioxide (SO_2), formaldehyde (HCHO), and aerosols, are retrieved in the ultraviolet (UV), visible (Vis), and near-infrared (NIR) spectral bands from nadir-viewing satellite instruments. NASA's Backscatter UV (BUV) instruments were the first satellite missions measuring total ozone columns since the 1970s (Mateer et al. 1971; Heath et al. 1975; Frederick et al. 1986; Bhartia et al. 2013). As shown in Table 1, satellites in low-Earth obit (LEO) provide a nearly daily global coverage and their spatial resolution has improved over time. Compared to GOME (1995–2011; Burrows et al. 1999), the GOME-2 series (2006–present; Munro et al. 2016) measure at four times higher spatial resolution, and the Ozone Monitoring Instrument (OMI; 2004–present; Veefkind et al. 2006) has a further improved spatial resolution (13×24 km^2). Measurements made by GOME, GOME-2, SCIAMACHY (2002–2012; Bovensmann et al. 1999), and OMI include important chemical species for atmospheric chemistry and have greatly advanced our understanding of air quality (e.g., Duncan et al. 2016; Levelt et al. 2018). TROPOMI (2017–present) onboard the Copernicus Sentinel-5 Precursor (Sentinel-5P) mission measures from UV-Vis-NIR to short-wave infrared (SWIR), which allows the measurements of an extended list of trace gases (Veefkind et al. 2012). Its unprecedented resolution of 3.5×5.5 km^2 and the high signal-to-noise ratio reveal enriched details of air pollution, which has greatly advanced air quality research in recent years (e.g., Fioletov et al. 2020; Stavrakou et al. 2020; Riess et al. 2022).

Infrared (IR) instruments also provide measurements about atmospheric composition. The MOPITT (Measurements Of Pollution In The Troposphere; 1999–present; Drummond et al. 2022; Buchholz et al. 2021) instrument measures carbon monoxide (CO) from the short-wave infrared and thermal infrared (TIR), and was one of the first satellite instruments that tracked global pollution transport. The Infrared Atmospheric Sounding Interferometer (IASI; 2006–present; Clerbaux et al. 2009) instruments were launched on the Metop (Meteorological Operational satellite) series, measuring meteorological variables, air pollutants, and greenhouse gases from the TIR with a 12 km footprint resolution. To date, 33 chemical species have been detected above the IASI instrumental noise level (Clarisse et al. 2011; Franco et al. 2018). As a companion to IASI, a series of TIR instruments have been launched by NASA and NOAA, the Atmospheric Infrared Sounder (AIRS; 2002–present; Lambrigtsen et al. 2004) on Aura, and NOAA's Cross-track Infrared Sounder (CrIS; 2011–present; Han et al. 2013).

Nadir-viewing LEO satellites provide valuable information on the seasonal and interannual variability of atmospheric composition. Rapid changes in emissions are detected, often in real-time, as demonstrated during the lockdowns in response to the COVID-19 spread (Bauwens et al. 2020; Liu et al. 2020a; Gkatzelis et al. 2021, among others). The LEO satellites provide decades of atmospheric composition measurements since the 1990s, allowing trend analysis at different spatial scales (e.g., Lamsal et al. 2015; Duncan et al. 2016; Stavrakou et al. 2018; Hedelius et al. 2021).

b. GEO satellites for atmospheric chemistry

Atmospheric composition measurements from GEO satellites greatly expand the global observing system for air quality. They can provide continuous observations during daytime hours (24 hours

TABLE 1. Constellation of nadir-viewing LEO and GEO space-borne atmospheric chemistry monitoring instruments since 2000.[a]

Satellite	Instrument	Operation period	Spectral range	Resolution (km^2)	Coverage[b]	Covered region
LEO						
ERS-2	GOME	1995–2011	UV-Vis	40×320	3 days	Global
Envisat	SCIAMACHY	2002–2012	UV-Vis-SWIR	30×60	6 days	
Aqua	AIRS	2002–present	TIR	13.5×13.5	0.5 day	
Terra	MOPITT	1999–present	NIR-TIR	22×22	5 days	
Metop	GOME-2	2006–present	UV-Vis	40×80	1.5 days	
	IASI		TIR	12×12[c]	0.5 day	
Aura	OMI	2004–present	UV-Vis	13×24	1 day[d]	
JPSS[e]	OMPS	2012–present	UV-Vis	10×10[f]	1 day	
	CrIS		TIR	14×14	0.5 day	
Sentinel-5P	TROPOMI	2017–present	UV-Vis-NIR-SWIR	3.5×5.5[g]	1 day	
Metop-SG A	IASI-NG	*2025*	TIR	12×12[c]	0.5 day	
	Sentinel-5		UV-Vis-NIR-SWIR	7.5×7.5	1 day	
GEO						
GK2B	GEMS	2020–present	UV-Vis	3.5×7.7 at 37.5°N	1 hour	East Asia
Intelsat 40e	TEMPO	2023–present	UV-Vis	2.1×4.5 at 36.5°N	1 hour	North America
MTG-S	Sentinel-4	*2025*	UV-Vis-NIR	8×8 at 45°N	1 hour	Europe and North Africa
	IRS		TIR	4×4 at nadir	1 hour[h]	Europe and Africa
Himawari[i]	AHI	2015–present	Vis-IR	2×2 at nadir	10 minutes[k]	East Asia, Southeast Asia and Oceania
FengYun-4	AGRI	2016–present	Vis-IR	2×2 at nadir	15 minutes[k]	Asia, Southeast Asia and Oceania
	GIIRS		TIR	12×12[l] at nadir	1.5 hours[m]	
GOES[j]	ABI	2017–present	Vis-IR	2×2 at nadir	10 minutes[k]	Western Hemisphere
GeoXO	ACX	*2035*	UV-Vis	8×4 at nadir	1 hour	North America
	GXS		TIR	4×4 at nadir	30 minutes[n]	Western Hemisphere

[a] Instruments dedicated to measuring GHGs are not considered within the scope of the paper. [b] Time required for global coverage for LEO instruments or coverage of the field of regard for GEO instruments. [c] IASI and IASI-NG have a circular pixel geometry of 12 km diameter. [d] The revisit time of OMI was increased to 2–3 days since 2018 due to the OMI row anomaly (Torres et al. 2018). [e] CrIS and OMPS are currently on the Suomi NPP, NOAA-20 and NOAA-21 satellites. They will also fly on the JPSS-3 and -4 satellites. [f] Pixel size of OMPS mapper on Suomi NPP is 50×50 km^2 but improved to 17×13 km^2 on NOAA-20 and then 10×10 km^2 on NOAA-21. OMPS nadir profiler has 250×250 km^2 resolution. [g] Resolution of TROPOMI at nadir observations was increased from 3.5×7 km^2 to 3.5×5.5 km^2 on 6 August 2019. [h] IRS revisit time is 30 minutes over Europe and 1 hour elsewhere. [i] The Advanced Himawari Imager (AHI) is operational on Himawari-8 and Himawari-9. [j] The Advanced Baseline Imager (ABI) is operational on GOES-16, GOES-17, GOES-18, and GOES-19. [k] ABI and AHI scan the full disk of observational coverage every 10 minutes. AGRI scans the full disk every 15 minutes. All three instruments support regional scans at 5 minutes or higher frequencies. [l] Pixel size is 16×16 km^2 for GIIRS on FengYun-4A and is 12×12 km^2 for GIIRS on FengYun-4B. [m] Time required to scan the field of regard is 2 hours for GIIRS on FengYun-4A and is 1.5 hours for GIIRS on FengYun-4B. [n] GXS scans the full disk of observational coverage every 30 minutes. It can also scan the contiguous United States every 15 minutes or scan mesoscale regions every 5 minutes.

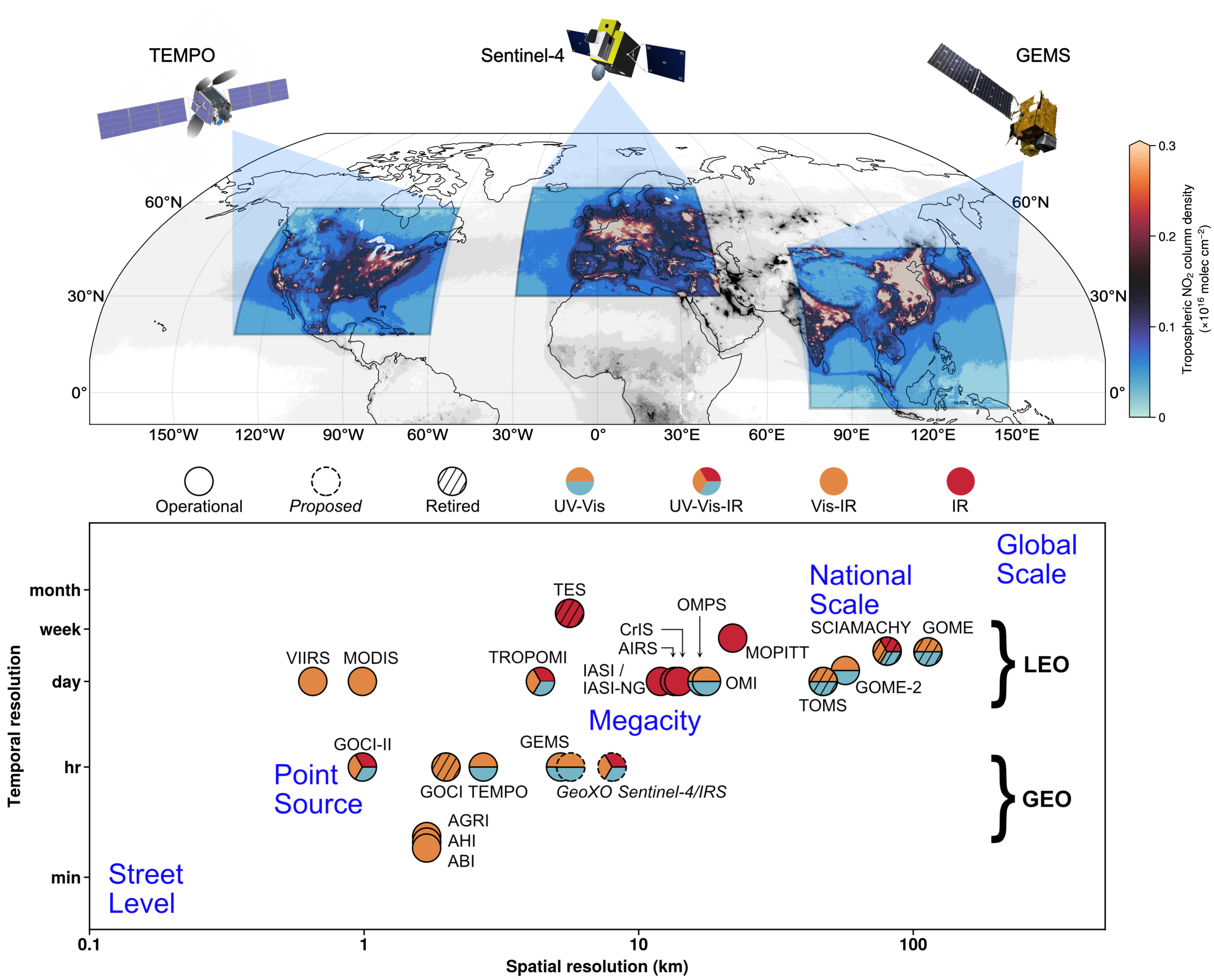

FIG. 1. (Top) Domain and coverage of the GEO satellites. Background is annual mean TROPOMI NO_2 tropospheric columns in 2022. Regions not covered by the GEO satellites are shaded in gray. (Bottom) Spatial and temporal resolution of space-borne instruments for atmospheric composition measurements. Figure adapted from Fig. 1 in Kim et al. (2020).

in the TIR). The geostationary orbit is 36 000 km from the Earth, as compared to ~500 km for LEO, but the weaker photon flux is compensated by a long staring capability so that pixel sizes and precisions from LEO and GEO atmospheric composition instruments are comparable. The same suite of species observable from LEO is also observable from GEO but with much higher data density over the field of regard. The field of regard for a geostationary instrument can be as large as one third of the Earth, although smaller domains are used in the geostationary air quality constellation (see Figure 1) to increase data density and achieve finer pixel resolution.

Geostationary satellites observe from fixed longitudes in an equatorial plane, which means that they have highest resolution at the Equator and limited observation capability for latitudes poleward of 60 degrees.

The Geostationary Interferometric Infrared Sounder (GIIRS) onboard China's FengYun-4 satellite series (FY-4A/B) is the first GEO hyperspectral infrared sounder. FY-4A and FY-4B currently operate at 86.5°E and 105°E, respectively. The GIIRS observations cover most of East Asia with a focus on China, with a 2-hour observing cycle. GIIRS measures at a 12 km spatial resolution at nadir and was recently used to retrieve ammonia (NH_3; Clarisse et al. 2021; Zeng et al. 2023b), CO (Zeng et al. 2023a), and formic acid (HCOOH; Zeng et al. 2024). The GIIRS onboard FY-4B (GIIRS/FY-4B; 2021–present) demonstrates improved sensitivity, better spatial resolution, and higher accuracy compared to GIIRS/FY-4A (2016–present;Yang et al. 2017). FY-4A/B also carry the Advanced Geostationary Radiation Imager (AGRI) that measures in Vis and IR.

GEMS is the first component of the GEO air quality constellation (see Fig. 1) and measures aerosols, O_3, NO_2, SO_2, HCHO, and glyoxal (CHOCHO), over Asia. It measures in UV-Vis with a spectral resolution of 0.6 nm and a spatial resolution of 3.5 km (NS) × 7.7 km (EW) at Seoul. It operates above 128.2°E, covering a field of regard from east of Japan to western India (75–145°E) and from Mongolia to Indonesia (45°N–5°S). GEMS is the first satellite observing the diurnal variation of air pollution in Asia, including urban pollution, power plants, industrial activities, ship emissions, wildfires, Asian dust, and volcanic eruptions. Figure 2A shows tropospheric NO_2 columns measured by GEMS for July 2023. Asian megacities are observed as pollution hot spots. The diurnal column variations of tropospheric NO_2 columns in Seoul, Beijing and New Delhi show large disparities due to regional differences in emissions, chemistry, and transport (see Figure 2C).

NASA's first Earth Venture Instrument (EVI), TEMPO is hosted onboard the Intelsat-40e satellite operating above 91°W. Compared to GEMS, TEMPO has a similar spectral resolution and an additional Vis-NIR channel to enhance retrieval sensitivity for tropospheric O_3 (Zoogman et al. 2017) and aerosols (Chen et al. 2021a). TEMPO scans North America from east to west hourly with a spatial resolution of 2.1 km (NS) × 4.75 km (EW) at the center of the field of regard (see Figure 2). TEMPO started its nominal operation in October 2023. The Beta version of data products was released on NASA's Atmospheric Science Data Center (ASDC) in May 2024 (see Table 2). Figure 2 shows TEMPO tropospheric NO_2 columns with marked pollution hot spots including the Northeast Corridor, the Canadian oil sands, and the Los Angeles Basin. The observed diurnal variations of tropospheric NO_2 in New York City and Los Angeles for 17–24 December 2023 show large regional differences as seen by GEMS (see Figure 2B). TEMPO can also measure the spectral signatures of nighttime lights and differentiate lighting types (Carr et al. 2017).

c. Future missions

The Copernicus Sentinel-4 mission will cover Europe, parts of North Africa and parts of the Atlantic (see Figure 1) centered at a fixed longitude of 0 degrees, with an hourly measuring frequency similar to GEMS and TEMPO. The operational products include NO_2, O_3, SO_2, aerosols, as well as the VOC (Volatile Organic Compound) tracers HCHO and CHOCHO. The first Meteosat Third Generation Sounder (MTG-S1) satellite, expected to be launched in 2025, will carry a Sentinel-4 instrument on board as well as the Infra-Red Sounder (IRS) (Coopmann et al. 2023). The IRS has an observational coverage including the entire Africa and Europe. It will measure every 30 minutes above Europe, and one hour elsewhere in the field of regard, which could be useful for species with a strong diurnal variability such as NH_3 (see Clarisse et al. 2023).

The Geostationary eXtended Observations (GeoXO) mission, NOAA's next generation GEO constellation covering the Western Hemisphere, is scheduled for launch in the early 2030s (Lindsey et al. 2024). The central GeoXO platform (operating above $\sim$105°W) will carry an atmospheric composition instrument (ACX) in the UV-Vis, as well as a hyperspectral IR sounder (GXS) for measurements of CO, NH_3, isoprene, and other VOCs. GeoXO will also carry an imager on board, similar to the Geostationary Operational Environmental Satellites-16 (GOES-16) Advanced Baseline Imager (ABI) currently used in various applications. For example, Zhang et al. (2022) and O'Dell et al. (2024) estimated surface particulate matter ($PM_{2.5}$) concentrations using aerosol optical depth measurements from GOES-16 and GOES-17. Watine-Guiu et al. (2023) also showed the potential of using the GOES constellation to monitor methane point sources.

IASI-new generation (IASI-NG, Clerbaux and Crevoisier 2013; Crevoisier et al. 2014) is the follow-on program for IASI, which will be flown onboard the Metop Second Generation (Metop-SG) satellites. The first Metop-SG platform is planned to be launched in 2025 to LEO and will also carry the Copernicus Sentinel-5 mission. IASI-NG will have higher spectral resolution and signal-

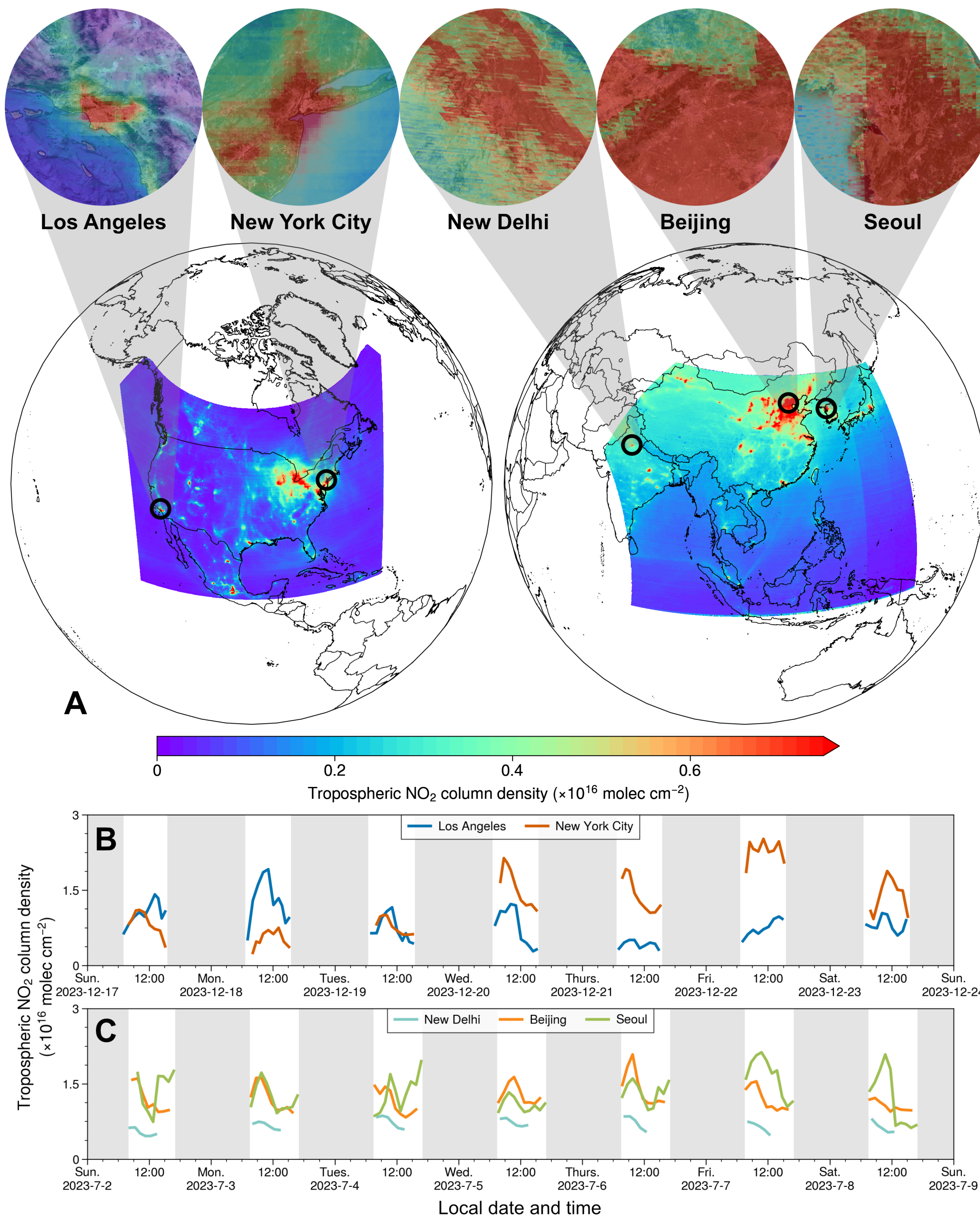

FIG. 2. (A) Illustration of tropospheric NO_2 column densities measured by TEMPO (left) and GEMS (right). Tropospheric NO_2 column densities measured over selected cities are shown on top. (B and C) Hourly tropospheric NO_2 column density measurement show diurnal and weekly cycles over large cities. The TEMPO data set used in this figure is preliminary and unvalidated, and is used for illustration purposes only.

to-noise ratio relative to IASI, providing better sensitivity near the surface and an improved vertical resolution of retrievals. Detection of weak absorbers (e.g., NH_3 and SO_2) will also improve.

3. Advances in air quality research using space-borne measurements

Over the past few decades, advances in atmospheric composition satellites have set the stage for air quality research and emission monitoring. The wealth of space observations has driven progress across all aspects of the research process. In this section, we provide an overview of recent advances in satellite-based air quality research. In Section 3.a, we review recent progress in the retrieval of atmospheric composition abundances from satellite measurements. In Sections 3.b and 3.c, we introduce efforts to improve emission estimation and data assimilation techniques, respectively. Finally, in Section 3.d, we discuss the applications of machine learning in air quality research.

a. Improved retrieval algorithms

Technological innovations and increasing quality requirements are driving the science of satellite retrievals forward. For example, significant improvements have been made on retrieval algorithms for TROPOMI since its launch in 2017, with a focus on better constrained uncertainties and reduced biases (Theys et al. 2021; Heue et al. 2022; Van Geffen et al. 2022, among others). Besides an improved degradation correction (Ludewig et al. 2020) and better consistency among retrieval products (Tilstra et al. 2024), new retrievals from TROPOMI measurements were developed, e.g., solar induced fluorescence (SIF; Guanter et al. 2021), aerosol optical depth (Torres et al. 2020), glyoxal (CHOCHO; Alvarado et al. 2020; Lerot et al. 2021), and nitrous acid (HONO; Theys et al. 2020). An overview of key air pollutants retrieved from space measurements is shown in Table 2.

The TROPOMI data products are carefully validated and validation reports are released regularly. As such, TROPOMI has been used as the reference and transfer standard for the development of GEMS retrieval algorithms. The first evaluation of GEMS retrievals using TROPOMI and ground-based measurements showed a good consistency (Baek et al. 2023; Kim et al. 2023). GEMS measurements captured clear seasonal variations over cities, as well as hourly variations that are also seen in ground-based remotely sensed columns (Lee et al. 2024). The list of GEMS retrievals

Table 2. Air pollutants retrieved from operational space-borne instruments, with DOIs to data products or references

Instruments	NO_2	O_3	SO_2	VOC		Aerosols	HONO	CO	NH_3
LEO									
TROPOMI	10.5270/S5P-9bnp8q8	10.5270/S5P-hcp1l2m	10.5270/S5P-74eidii	**HCHO**	10.5270/S5P-vg1i7t0	10.5270/S5P-7g4iapn	10.18758/71021058	10.5270/S5P-bj3nry0	**Not measured**
				CHOCHO	10.18758/4oaroxyf				
OMI	10.5067/Aura/OMI/DATA2018	10.5067/Aura/OMI/DATA2013	10.5067/Aura/OMI/DATA2023	**HCHO**	10.5067/Aura/OMI/DATA2015	10.5067/Aura/OMI/DATA2001	**Not measured**		
GOME-2	Available at EUMETSAT Satellite Application Facility on Atmospheric Composition Monitoring (AC SAF)						**Not measured**		
IASI	**Not measured**	Available at AERIS atmospheric data center					10.5281/zenodo.10721381	Available at AERIS	
OMPS	10.5067/N0XVLE2QAVR3	10.5067/0WF4HAAZ0VHK	10.5067/A9O02ZH0J94R	**HCHO**	10.5067/IIM1GHT07QA8	10.5067/40L92G8144IV	**Not measured**		
CrIS	**Not measured**	10.5067/WUKWENW76N5P	Hyman and Pavolonis (2020)	**HCHO**	Fu et al. (2019)	**Not measured**		10.5067/BYIIUV3PR9L6	10.5067/7I3KMUCCJNEN
Other LEO satellites	**Not available**	TES: 10.5067/AURA/TES/TL2O3N.008	MLS: 10.5067/Aura/MLS/DATA2519	**Not available**		VIIRS: 10.5067/VIIRS/AERDB_L2_VIIRS_SNPP.002	**Not available**	MOPITT: 10.5067/TERRA/MOPITT/MOP03JM.009	AIRS: 10.5067/EYXLPVGTSWFF
GEO									
GEMS	Available from National Institute of Environmental Research, Environmental Satellite Center						**Not available**	**Not measured**	
TEMPO	10.5067/IS-40e/TEMPO/NO2_L2.001	10.5067/IS-40e/TEMPO/O3TOT_L2.003	**Not available**	**HCHO**	10.5067/IS-40e/TEMPO/HCHO_L2.001	**Not available**	**Not measured**		
FY-4A/B (GIIRS)	**Not measured**			**Not available**		Available from Fengyun Data Center	**Not measured**	10.18170/DVN/M7DKKL	10.18170/DVN/VJ4MLO

was recently extended to SO_2 (Park and Jeong 2021), aerosols (Cho et al. 2023; Park et al. 2023), and glyoxal (Ha et al. 2024).

Continued efforts to improve retrieval algorithms have led to new data products for older missions like OMI, e.g., SO_2 (Li et al. 2022) and O_3 (Bak et al. 2024). Thermal infrared measurements are now better utilized to monitor extreme events, such as wildfires (Vu Van et al. 2023; Luo et al. 2024) and volcanic activities (Taylor et al. 2018). Notably, the phenomenal 2022 Hunga Tonga–Hunga Ha'apai eruption was well observed by thermal infrared spectrometers (e.g., Wright et al. 2022). The IASI NH_3 and ethylene (C_2H_4) retrievals were used to identify point sources from industrial and agricultural sectors (Van Damme et al. 2018; Franco et al. 2022).

The signal-to-noise ratio remains a limiting factor for the retrieval of weakly-absorbing trace gases (e.g., formaldehyde, SO_2, and NH_3). Some recent studies average satellite measurements over longer time periods to obtain a significant signal (e.g., Van Damme et al. 2018). For more strongly absorbing gases, like NO_2, sources of retrieval uncertainties include surface reflectivity, clouds and aerosols, and aspects like thermal contrast for infrared measurements. Atmospheric profiles have a strong impact on retrievals in the UV-Vis due to the altitude dependency of Rayleigh scattering, which becomes more important as the spatial resolution increases (Lamsal et al. 2021). Averaging kernels have been used in the validation of retrievals and data assimilation to account for the information content of the retrievals (Eskes and Boersma 2003).

To use satellite data at a higher spatial resolution, new oversampling methods have been developed (Valin et al. 2013; Fioletov et al. 2015; Sun et al. 2018; Van Damme et al. 2018; Clarisse et al. 2019, among others). For retrievals over emission hotspots, the assumptions about the vertical distribution of gases (averaging kernels and air mass factors) are particularly important for the quantification of tropospheric amounts and diurnal variations (Yang et al. 2023b). Regional models capable of achieving 10 km resolution are being used to provide a priori information for high-resolution retrieval products (e.g., Liu et al. 2020b for NO_2 in Asia, and Douros et al. (2023) for NO_2 in Europe).

b. Estimation of emissions

The development of emission inventories remains challenging due to the large number of species taken into account, the variety of emission sources, and because the a priori information is typically collected by networks that are spatially and temporally sparse (Granier et al. 2023; Sindelarova et al. 2023). For instance, the activity data and emission factors for anthropogenic emissions are available from diverse agencies, such as the International Energy Agency, but public access to this information is often limited. The development of open-source databases has been led by intergovernmental organizations, e.g., the Intergovernmental Panel on Climate Change Emissions Factor Database (IPCC EFDB) or the United Nations Framework Convention on Climate Change (UNFCCC), both of which are built on the data released in national reports. Global emission inventories are generally available with a delay of three to four years. To support policy-making and air quality applications, techniques have been developed to extrapolate emissions to the most recent years (Soulie et al. 2023). The development of emission inventories also need to incorporate a finer temporal resolution and detailed categorization by specific emission sectors. To this end, temporal profiles based on statistical information (e.g., traffic counts) and meteorological parametrizations are typically considered (e.g., Guevara et al. 2021). Additional constraints on temporal profiles can be obtained from the hourly GEO observations, especially the diurnal variations of emissions (Park et al. 2024). Table 3 lists the main publicly available emission inventories, covering both pollutants and greenhouse gases at global and regional scales.

Large discrepancies have been highlighted among emission inventories due to differences in the activity data and emission factors (Elguindi et al. 2020; Granier et al. 2023). Complementary to the emission inventories, a growing number of studies (cf. Section 3.c) use satellite observations and inverse modeling techniques to estimate emissions, namely NOx (e.g., Stavrakou et al. 2008; Kurokawa et al. 2009; Miyazaki et al. 2017; Jiang et al. 2022; Plauchu et al. 2024; van der A et al. 2024), VOCs (e.g., Millet et al. 2008; Stavrakou et al. 2012; Marais et al. 2012; Bauwens et al. 2016; Cao et al. 2018; Oomen et al. 2024; Müller et al. 2024), CO (e.g., Arellano et al. 2004; Müller et al. 2018; Qu et al. 2022b) and greenhouse gases (e.g., Wang et al. 2018; Lu et al. 2021). Figure 3 illustrates a comparison of NOx emissions in China from 2000 to 2020 from several emission inventories and satellite-based emission estimates (Elguindi et al. 2020). The differences between various estimates remain significant, especially for the trends, which underscores the need for continued efforts on mitigating uncertainties in emissions.

The development of new retrievals (see Section 3.a) has advanced emission estimates from both natural and anthropogenic sources. For example, the new TROPOMI HONO retrieval product

TABLE 3. List of several global and regional publicly available emissions inventories

Acronym	Time period covered	Spatial resolution (degree^2)	Temporal resolution	Species considered	DOI or reference
Global inventory					
EDGARv8	1970–2022	0.1x0.1	Monthly	Pollutants+GHGs	Crippa et al. (2023a, 2024)
HTAPv3	2000–2018	0.1x0.1	Monthly	Pollutants	Crippa et al. (2023b)
CEDS	1980–2019	0.1x0.1	Monthly	Pollutants+GHGs	10.25584/PNNLDH/1854347
CAMS-GLOB-ANT v6.2	2000–2025	0.1x0.1	Monthly	Pollutants+GHGs	10.24380/eets-qd81
ECLIPSE v6	1990–2050 (by 5 or 10 yrs)	0.5x0.5	Yearly	Pollutants+CH_4	Klimont et al. (2017)
Regional inventory					
CAMS-REG (Europe)	2000–2022	0.1x0.05	Yearly	Pollutants+GHGs	Kuenen et al. (2021)
EMEP (Europe)	1990–2022	No grid	Yearly	Pollutants	European Environment Agency (2023)
EPA[a] (USA)	1970–2023	No grid	Yearly	Pollutants+GHGs	epa.gov
Government Canada	1990–2022	No grid	Yearly	Pollutants+GHGs	Environment and Climate Change Canada (2019); Government of Canada (2018)
PAPILA (Latin America)	2014–2020	0.1x0.1	Yearly	Pollutants+GHGs	10.5281/zenodo.12944491
DACCIWA (Africa)	1990–2015	0.1x0.1	Yearly	Pollutants	Keita et al. (2021)
MIXv2 (Asia)	2010–2017	0.1x0.1	Monthly	Pollutants+CO_2	Li et al. 2023b
REASv3.2 (Asia)	1950–2015	0.25x0.25	Monthly	Pollutants+CO_2	Kurokawa and Ohara (2020)
MEIC 1.4 (China)	1990–2020	0.25x0.25	Monthly	Pollutants+CO_2	Zheng et al. (2018)

[a] Table shows the EPA Air Pollutant Emissions Trends Data. The EPA National Emissions Inventory (NEI) are available every three years with variable resolutions from 36 km to 4 km.

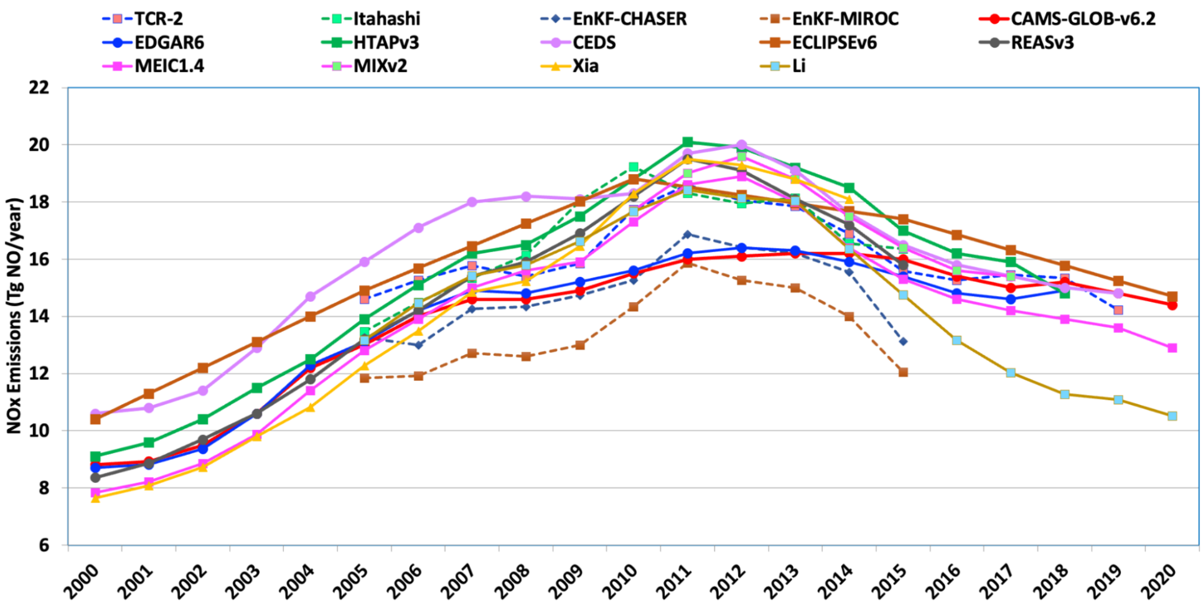

FIG. 3. Comparison of annual mean NOx emissions in China from 2000 to 2020 (in Tg NOx-NO/yr) from several datasets. Solid and dashed lines represent emission inventories and satellite-based emission estimates, respectively. The references for the emission estimates are shown in the legend on top. Figure adapted from Elguindi et al. (2020).

shows intense emissions in wildfire plumes, accounting for a substantial share of total hydroxyl radical (OH) production from natural sources (Theys et al. 2020). The first global satellite isoprene retrievals from CrIS (Fu et al. 2019), combined with HCHO observations, have been used to constrain isoprene emissions and atmospheric oxidation (Wells et al. 2020). These analyses reveal significantly underestimated isoprene emissions in emission inventories, particularly in tropical regions (Wells et al. 2020). The use of satellite retrievals has also proven to be crucial for identifying seasonalities and weekly patterns in emissions, providing complementary information to temporal profiles derived from activity data. This is particularly valuable for sources with limited activity information, such as those in the agricultural sector (e.g., Damme et al. 2022). Wind rotation method is another important advancement that estimates point source emissions by resolving emission plumes aligned with the wind direction (e.g., Beirle et al. 2011; Valin et al. 2013; Fioletov et al. 2015; Clarisse et al. 2019).

FIG. 4. Evolution of the spatial resolution of space-based NO_2 data assimilation studies over the past two decades. Orange symbols denote global studies, blue symbols denote regional studies. Circles describe data assimilation systems in which only NO_2 is assimilated. Squares represent multi-species data assimilation studies. The size of the symbol represents the temporal scale.

c. Advances in data assimilation

Data assimilation in air quality research combines observations with chemical transport models (CTMs) to produce an analysis of the state of atmospheric composition (e.g., Carmichael et al. 2008; Lahoz and Schneider 2014). Areas of application include air quality forecasting (e.g., Inness et al. 2015), inverse modeling of emissions and other model parameters, and constructing reanalyses of atmospheric composition. Numerous advances have been achieved in data assimilation in the past decades, owing to improved satellite retrievals, better parameterized models, and advanced assimilation techniques (Sandu and Chai 2011; Streets et al. 2013; Bocquet et al. 2015). For examples shown in Figure 4, the assimilation of space-based NO_2 data has evolved to increasingly high spatial resolution in recent years.

Data assimilation techniques solve for the statistically optimal solution based on observations and models (Kalnay et al. 2007). Filtering approaches such as the ensemble Kalman filter (EnKF) capture chemical non-linearities using an ensemble of models and estimate emissions at regional (Tang et al. 2013; Yumimoto et al. 2014; Gaubert et al. 2020; Feng et al. 2020; Dai et al. 2021; van der Graaf et al. 2022) and global (Miyazaki et al. 2012, 2020a; Gaubert et al. 2023) scales. The 4D-Var method utilizes the adjoint of forward models to minimize the model-observation mismatch. Although the development of adjoint models can be complex and running them can be computationally costly, 4D-Var has been successfully implemented for various applications (Elbern et al. 2000; Müller and Stavrakou 2005; Henze et al. 2007). 4D-Var is also used in the Integrated Forecasting System (IFS) of the European Union's Copernicus Atmosphere Monitoring Service (CAMS) (Inness et al. 2015, 2019, 2022).

Simultaneous joint assimilations of multiple species, such as CO/NO_2 (Müller and Stavrakou 2005), HCHO/CHOCHO (Stavrakou et al. 2009; Cao et al. 2018), SO_2/NO_2 (Qu et al. 2019; Wang et al. 2020), and $NO_2/CO/SO_2$ (Miyazaki et al. 2017, 2020a,b), have shown to improve data assimilation results, as it accounts for the impact of emission changes on the chemical lifetimes of various species. Specifically, assimilating short-lived species can help better characterize the budget of longer-lived gases (e.g., Gaubert et al. 2017; Zheng et al. 2019). To address the increased computational cost of multi-species data assimilation, hybrid approaches combining 3D-Var and mass balance have been recently developed to improve the computational efficiency (Li and Xiao 2019; Chen et al. 2021b).

d. Application of machine learning

Machine learning has recently become a popular choice for satellite retrievals due to its higher computational efficiency with respect to traditional retrieval methods. One of the first machine learning applications widely used in data products is the operational IASI NH_3 retrievals based on neural networks (Whitburn et al. 2016; Van Damme et al. 2017). Following that, new data products have been developed for IASI, e.g., the acetone and ethylene retrievals (Franco et al. 2019, 2022), and the CrIS data products (Wells et al. 2022, 2024).

An emerging application of machine learning studies is the estimation of surface concentrations using neural networks and tree-based models for $PM_{2.5}$ (Di et al. 2019; Wei et al. 2020; Pendergrass et al. 2022), O_3 (Sayeed et al. 2021; Betancourt et al. 2022), NO_2 (Di et al. 2020; Ghahremanloo et al. 2021; Chan et al. 2021), CO (Han et al. 2022; Chen et al. 2024), and CH_4 (Balasus et al. 2023). These studies rely on the fusion of data from multiple sources and show improved skill compared to conventional approaches (Balasus et al. 2023; Oak et al. 2024; Huang et al. 2024). Other research directions include the development of surrogate models or modules in conventional modeling systems with an improved efficiency (Keller and Evans 2019; Kelp et al. 2020, 2022; He et al. 2024b). Using machine learning to understand drivers of air pollution (Zhang et al. 2023; Ma et al. 2023; Wang et al. 2024) and conduct trend analysis (He et al. 2022a; Pendergrass et al. 2022, 2024; Li et al. 2023a) are other intriguing directions. The potential of machine learning in the inverse modeling of emissions has also been explored (Huang et al. 2021; He et al. 2022b).

4. Challenges and opportunities in the era of geostationary space observations

Space observations from GEO offer a number of opportunities for improved characterization of air quality and emissions as compared to LEO observations. The higher observation density due to more frequent return times allows for higher precision. It also facilitates cloud clearing, meaning an increased probability of observing a cloud-free scene in a certain location (or adjacent locations) over a certain time period. The continuous observation available from GEO instruments enables the tracking of pollution transport on meso- and synoptic scales. Multiple measurements during the day provide information on the diurnal variations of emissions and chemical evolution. However, there are also important challenges in the retrieval and the interpretation of GEO observations. Next, we elaborate on the opportunities and challenges in retrieval development (Section 4.a), atmospheric composition modeling (Section 4.b), data assimilation (Section 4.c), and machine learning applications for GEO observations (Section 4.d), and we discuss air quality research for large world regions that are not covered by the planned GEO satellite constellation (Section 4.e).

a. Retrievals

For GEO observations, not only do the pollutant concentrations change over the day, but the position of the Sun, the surface temperature, the vertical mixing of the atmosphere, and meteorology also change. These parameters are either input variables or impact the a priori vertical profile of the trace gases being retrieved, of which the hourly variations need to be accounted for in retrieval algorithms.

An important aspect is the variation in surface reflectivity for UV-Vis retrievals. Larger reflectivity increases the sensitivity of satellite measurements to trace gases close to the surface, and not considering the diurnal variations in surface reflectivity could lead to artifacts in the retrieved diurnal variation of pollutants. While surface reflectivity information is available from satellite observations, the temporal and spatial resolution may not be sufficient, and uncertainties can be large for individual observations. A similar problem exists for TIR retrievals, where surface radiation emission is strongly dependent on temperature.

A second challenge is the diurnal variation due to vertical mixing, which can change the sensitivity of the satellite measurements to different vertical layers in the atmosphere (Yang et al. 2023a). For UV-Vis retrievals, sensitivity is usually lowest close to the surface, and a shallow boundary layer in the morning reduces sensitivity compared to a fully developed boundary layer in the afternoon. The situation can further be complicated by residual aerosols above the boundary layer. Similar issues are expected from the combination of vertical trace gas distributions and temperature profiles for TIR observations. To account for these effects, atmospheric models used as a priori information in retrievals must reflect the diurnal evolution of the boundary layer, which can be challenging over complex urban areas and terrain.

The viewing geometry from GEO can also present challenges, especially for higher latitudes and at the edges of the field of regard. For UV-Vis observations, large viewing zenith angles can lead to increased scattering in the atmosphere and reduced sensitivity to trace gases near the surface. The effect is further amplified by the presence of aerosols and clouds. In addition, spatial oversampling is generally of limited use for GEO observations due to the constant ground pixel pattern, as reported in Lange et al. (2024) for the case of GEMS. A possible solution would be to adjust the latitudinal pointing and longitudinal sampling of GEO measurements, but this may complicate the interpretation of the observed diurnal variations and affect the aerosol and cloud measurements, which depend on accurate surface reflectance characterization.

For some trace gases, such as O_3 and NO_2, significant amounts are present in both the troposphere and the stratosphere. This necessitates a stratospheric correction, which, in the case of GEO observations, also needs to account for the diurnal change of the stratospheric amounts. This is particularly relevant for small signals, which are more affected by uncertainties in the stratospheric correction.

Given the challenges outlined above, robust calibration and validation of GEO observations becomes essential to ensure a consistent retrieval quality across different sensors and GEO regions. The calibration and validation efforts for GEO observations will build on the experience from heritage LEO missions (CEOS 2019). These efforts should be supplemented by intensive ground-based and aircraft validation campaigns to evaluate the diurnal patterns measured by the GEO satellites (see e.g. Kim et al. 2023; Lee et al. 2024; Lange et al. 2024; Ha et al. 2024). LEO air quality missions will serve as a traveling standard for the inter-comparability of the different GEO instruments. Further efforts should focus on the development of an harmonized framework for the processing, validation, and publication of all data products from the constellation of GEO composition observations (CEOS 2019).

The availability of multiple measurements per day also provides opportunities for improved retrieval techniques. For example, the nearly simultaneous observation of contiguous scenes facilitates cloud slicing, where differences in column amounts above optically thick clouds are used to provide information on vertical distribution (Marais et al. 2021). Imagers and spectrometers on GEO platforms, combined with LEO missions, will deliver measurements of multiple chemical species over emission hotspots across a broad spectral range. This expanded coverage has the potential to enable the retrieval of new information and deepen our understanding of emission activities.

b. Modeling

GEO composition observations will be useful for the evaluation of high-resolution regional and local chemical transport models, and specifically to compare calculated diurnal variations with the hourly data provided by the retrievals. The measured variations in column concentrations may be very different from the time evolution of surface concentrations (e.g., Tang et al. 2021). A full understanding of the observed diurnal variation is not straightforward because, in addition to the time-evolving forcing from solar radiation, it is driven by other factors such as local emissions, boundary layer meteorology, etc. (Edwards et al. 2024). One challenge is to improve the representation of small-scale dynamical features in the planetary boundary layer, including the formation of the heat island in urban areas, the development of convective cells and local cloudiness, the impact of topography and buildings on the small-scale flow, and the influence of diurnal varying coastal circulation cells.

Regional chemical-meteorological models at a spatial resolution of typically 1 to 5 km are used to provide background information on the chemical composition; they are now often complemented by numerical simulations of large eddies in the boundary layer in order to resolve their impact on the reaction rates and on chemical segregation associated with emission heterogeneity in a complex urban canopy (Wang et al. 2022). Street network models such as the MUNICH model (Kim et al. 2018) provide the distribution of chemically reactive pollutants along street canyons. The success of such approaches depends on the availability of detailed high-resolution (better than 1 km) emission inventories, which are usually not yet available.

Recent efforts have led to the development of global multi-scale models with grid refinement capabilities over selected geographical regions. An irregular model grid with a grid refinement capability over the three regions covered by GEMS, TEMPO and Sentinel-4 has been developed as part of the next-generation community modeling infrastructure, MUSICA (the Multi-Scale Infrastructure for Chemistry and Aerosols; Pfister et al. 2020). Its purpose is to insert high-resolution regional information provided by the GEO satellites in a global modeling framework that accounts for large-scale transport and distant influences on chemical species (Pfister et al. 2020).

c. Data assimilation

There are several challenges related to the assimilation of GEO observations. The efficient assimilation of such dense observations will require high-resolution forecast models and appropriate data assimilation techniques, in addition to a flexible system handling multiple satellite sensors from both GEO and LEO. As summarized below, further innovations are needed to take advantage of GEO satellite observations with data assimilation.

(1) Parameter estimation: In tropospheric chemistry, boundary conditions, reaction rates, and emissions often play an important role, whereas the role of initial conditions is limited due to rapid chemical reactions (Sandu and Chai 2011; Goris and Elbern 2013). Dense observations from GEO satellites may allow for detailed parameter estimation beyond a few key chemical species, improved

sectoral emissions estimates (Qu et al. 2022a; Gaubert et al. 2023), and speciation information for VOCs and aerosols. They can also be used to correct for meteorological parameters such as horizontal wind (Liu et al. 2021).

(2) Data assimilation methodology: With greater observational coverage and high measurement accuracy, local emission sources could be estimated using computationally efficient approaches such as the mass balance approach (e.g., Cooper et al. 2017; Qu et al. 2019), or by making use of trajectories to describe the non-local relation between emissions and concentrations (e.g., van der A et al. 2024). Nevertheless, flow-dependent background covariance, including covariance among chemical species, is essential to integrate multiple-species information and their spatial distributions. DA techniques also need to account for diurnal changes in chemistry, emissions, and measurement characteristics (e.g., Timmermans et al. 2019; Shu et al. 2023). Efficient non-Gaussian methods such as particle filters may also be needed for high-resolution DA (Valmassoi et al. 2023).

(3) Plume analysis and emission estimates: The latest GEO and LEO satellite composition observations are able to resolve plumes of urban emissions, major point sources and even individual ships. Computationally efficient techniques such as plume fitting (e.g., Fioletov et al. 2017), the flux-divergence technique (e.g., Beirle et al. 2023), or the integrated mass enhancement method (e.g., Varon et al. 2018; He et al. 2024a) have been successful in providing emission estimates for short-lived and long-lived tracers at the instrumental resolution. A major challenge for short-lived compounds like NO_2 is to account for the non-linear chemistry in plumes, leading to a heterogeneous plume composition and lifetime (Krol et al. 2024), and to determine how these local effects impact global or regional data assimilation systems.

(4) Combination of multiple observing systems: LEO composition observations provide constraints on long-range transport (Miyazaki et al. 2022) and reduce model errors in regions constrained by GEO composition observations. Well-validated LEO data can be used to benchmark GEO composition observations, for example, as an anchor for DA bias correction. As the spatial resolution of both forecast models and satellites increases, assimilation of in situ and satellite observations will be another effective approach to improve analysis, especially near the surface. New technical challenges for simultaneous assimilation include appropriate background error co-

variance at multiple scales and error statistics including representative errors of each measurement (Wang and Wang 2023).

d. Machine learning

For future applications of machine learning in air quality research, the differences between LEO and GEO viewing geometries need to be accounted for. Solar zenith angle and viewing zenith angle could have greater importance when constructing machine learning models for retrieving atmospheric composition from GEO satellites. Diurnal variations in related physical parameters should also be captured by input variables for machine learning models for GEO composition satellites.

Recent applications of machine learning for LEO atmospheric composition satellites have focused on concentration estimation and the development of surrogate models. More efforts are needed in applying machine learning to inverse modeling of emissions. Specifically, further development of explainable machine learning models is necessary to enhance the interpretability and robustness of emission estimates.

Despite the challenges, geostationary atmospheric composition satellites offer opportunities to further advance innovation in future machine learning applications. For example, machine learning is effective in anomaly detection and pattern recognition, both making it well-suited for monitoring extreme events (e.g., wildfires and volcano eruptions). Its scalability to the high temporal and spatial resolution of GEO composition measurements can be critical for real-time decision-making and mitigating the impacts of extreme events.

The generalizability of machine learning is another key strength that enhances data fusion. Recent studies indicate that integrating multi-source measurements using machine learning can help reduce discrepancies between different datasets (Balasus et al. 2023; Oak et al. 2024; Huang et al. 2024). Integrating LEO composition measurements can play a critical role in improving the consistency of composition measurements made by different GEO satellites.

e. Atmospheric composition monitoring for other regions of the world

Space-borne instruments in LEO have been vital for addressing data sparsity in large parts of the world, in particular for the African and South American continents and parts of Asia. These regions will continue to rely on LEO instruments, as the planned GEO satellite constellation mainly covers the Northern Hemisphere (Paton-Walsh et al. 2022). The validation of both LEO and GEO observations and the derived products is also rare across the tropics and Southern Hemisphere. Such validation requires routine surface observations and aircraft campaigns to profile the troposphere under a range of representative conditions (Tang et al. 2023).

The Sentinel-4 GEO composition instrument will observe a portion of North Africa, and the IRS on the same platform will provide observations of infrared-absorbing compounds like CO and NH_3. CO observations over Africa will be vital for understanding inefficient combustion sources, including biomass burning for agricultural practices in Africa (Andreae 2019), burning of waste (Wiedinmyer et al. 2014), and from other inefficient combustion practices (Marais and Wiedinmyer 2016; Bockarie et al. 2020). High-frequency NH_3 observations are well timed to coincide with agricultural intensification that includes the use of synthetic nitrogen fertilizer and intensive livestock farming (Hickman et al. 2021). A demonstration of the utility of GEO observations of NH_3 and CO for informing diurnal changes in abundances, precursor emissions, and pollution transport patterns over Africa would aid in advocating for dedicated GEO instruments over Africa and South America. However, the long delay between mission concept and launch means missing out on advancing understanding in regions of the world during a period of unprecedented population growth and land use changes. An advisory committee comprising researchers, academics and satellite instrument developers has been formed to propose GEO missions over Africa and South America, but a greater representation of researchers from these regions is needed to inform the development of a fit-for-purpose mission (Marais and Chance 2015).

5. Conclusions and recommendations

The implementation of GEO satellites for atmospheric composition monitoring opens new perspectives for air quality research. The first two GEO composition satellites over Asia and North America have demonstrated the measurement of diurnal variation of chemical species, thereby providing unprecedented information on the diel evolution of emissions, photochemical processes and the effects of atmospheric dynamics over large regions. However, the development of retrievals and the validation of these GEO satellite composition data is still ongoing, as there is still room for improvement. Furthermore, the European component of the GEO constellation in Sentinel-4 is expected to be launched in 2025. The exploitation of measurements conducted by GEO satellites presents new challenges and several priority tasks can therefore be highlighted for future research.

- Retrieval algorithms need to be carefully adapted to the GEO composition observations. Specifically, the diurnal variations of various parameters used in the retrieval, such as surface reflectivity and vertical mixing, need to be resolved. Additionally, the viewing geometry can present difficulties due to the large zenith angles of GEO instruments compared to nadir-viewing satellites, hence correcting for these effects at the edges of the field of regard is necessary.

- The hourly temporal resolution of GEO observations gives crucial information on diurnal profiles of emissions of atmospheric pollutants. In order to leverage this aspect in emission inversion studies and reduce the delay in the delivery of emission inventories, temporal profiles for different sectors in emission inventories need to be provided.

- Global and regional models should be adapted to be more compatible with the GEO atmospheric composition satellites. Continuous model development, especially regarding the fine-scale chemical processes, is essential for retrievals, air quality forecasting, and data assimilation in the era of GEO satellites for atmospheric composition monitoring.

- Data assimilation methods need to be adapted to the geostationary case. Specifically, more computationally efficient methods should be explored in order to optimally process the high data volume. The co-existence of LEO and GEO measurements in the same area opens possibilities to assimilate both datasets simultaneously, along with ground-based and aircraft data. Deriving emissions from point sources from plume estimation methods also provides a promising avenue, considering the higher temporal resolution of observations.

- The computational efficiency and generalizability of machine learning make it a valuable area for further exploration. In addition to recent applications of machine learning in retrieval algorithm development and surface concentration estimation, greater efforts should be directed toward inverse modeling of emissions and the development of explainable models.

Finally, it is crucial to keep improving the accessibility of satellite measurements to agencies in charge of air quality management, especially for regions lacking the capability to establish observation networks. Future GEO satellites should provide data over Africa, South America, Southern Asia, Australia, New Zealand, and other regions not covered by the current observing capabilities.

Acknowledgments. This research was supported by the International Space Science Institute (ISSI) in Bern and Beijing, through ISSI/ISSI-Beijing International Team project #489 (Use of Geostationary Satellites to Improve Air Quality Characterization and Forecasts). This work is partially supported by a NASA Early Career Faculty Grant (80NSSC21K1808). A portion of this research was carried out at the Jet Propulsion Laboratory, California Institute of Technology, under a contract with the National Aeronautics and Space Administration (80NM0018D0004). The NSF National Center for Atmospheric Research is sponsored by the National Science Foundation (NSF).

The GEMS NO_2 tropospheric column density data are publicly available on request from the National Institute of Environmental Research (NIER) Environmental Satellite Center (ESC) (`https://nesc.nier.go.kr/en/html/datasvc/data.do?pageIndex=1&outputInnb=64&atrb=NO2_Trop`, last access: 3 August 2024). The TEMPO NO_2 tropospheric columns are openly available from the NASA Earthdata Atmospheric Science Data Center (`https://asdc.larc.nasa.gov/project/TEMPO/TEMPO_NO2_L2_V01` with DOI:`10.5067/IS-40e/TEMPO/NO2_L2.001`, last access: 3 August 2024). The TROPOMI monthly mean NO_2 tropospheric columns are available from the KNMI Tropospheric Emission Monitoring Internet Service (`https://www.temis.nl/airpollution/no2col/no2month_tropomi.php`, last access: 3 August 2024).

References

Alvarado, L. M. A., A. Richter, M. Vrekoussis, A. Hilboll, A. B. K. Hedegaard, O. Schneising, and J. P. Burrows, 2020: Unexpected long-range transport of glyoxal and formaldehyde observed from the copernicus sentinel-5 precursor satellite during the 2018 canadian wildfires. *Atmospheric Chemistry and Physics*, **20**, 2057–2072, https://doi.org/10.5194/acp-20-2057-2020.

Andreae, M. O., 2019: Emission of trace gases and aerosols from biomass burning – an updated assessment. *Atmospheric Chemistry and Physics*, **19**, 8523–8546, https://doi.org/10.5194/acp-19-8523-2019.

Arellano, A. F., P. S. Kasibhatla, L. Giglio, G. R. van der Werf, and J. T. Randerson, 2004: Top-down estimates of global co sources using mopitt measurements. *Geophysical Research Letters*, **31**, https://doi.org/10.1029/2003GL018609.

Baek, K., J. H. Kim, J. Bak, D. P. Haffner, M. Kang, and H. Hong, 2023: Evaluation of total ozone measurements from Geostationary Environmental Monitoring Spectrometer (GEMS). *Atmospheric Measurement Techniques*, **16**, 5461–5478, https://doi.org/10.5194/amt-16-5461-2023.

Bak, J., X. Liu, K. Yang, G. Gonzalez Abad, E. O'Sullivan, K. Chance, and C.-H. Kim, 2024: An improved omi ozone profile research product version 2.0 with collection 4 L1b data and algorithm updates. *Atmospheric Measurement Techniques*, **17 (7)**, 1891–1911, https://doi.org/10.5194/amt-17-1891-2024, URL https://amt.copernicus.org/articles/17/1891/2024/.

Balasus, N., and Coauthors, 2023: A blended TROPOMI+GOSAT satellite data product for atmospheric methane using machine learning to correct retrieval biases. *Atmospheric Measurement Techniques*, **16 (16)**, 3787–3807, https://doi.org/10.5194/amt-16-3787-2023, URL https://amt.copernicus.org/articles/16/3787/2023/.

Bauwens, M., and Coauthors, 2016: Nine years of global hydrocarbon emissions based on source inversion of OMI formaldehyde observations. *Atmospheric Chemistry and Physics*, **16 (15)**, 10 133–10 158, https://doi.org/10.5194/acp-16-10133-2016.

Bauwens, M., and Coauthors, 2020: Impact of coronavirus outbreak on NO_2 pollution assessed using TROPOMI and OMI observations. *Geophysical Research Letters*, **47**, https://doi.org/10.1029/2020GL087978.

Beirle, S., K. F. Boersma, U. Platt, M. G. Lawrence, and T. Wagner, 2011: Megacity emissions and lifetimes of nitrogen oxides probed from space. *Science*, **333 (6050)**, 1737–1739, https://doi.org/10.1126/science.1207824, URL https://www.science.org/doi/abs/10.1126/science.1207824, https://www.science.org/doi/pdf/10.1126/science.1207824.

Beirle, S., C. Borger, A. Jost, and T. Wagner, 2023: Improved catalog of NO_x point source emissions (version 2). *Earth System Science Data*, **15**, 3051–3073, https://doi.org/10.5194/essd-15-3051-2023.

Betancourt, C., T. T. Stomberg, A.-K. Edrich, A. Patnala, M. G. Schultz, R. Roscher, J. Kowalski, and S. Stadtler, 2022: Global, high-resolution mapping of tropospheric ozone – explainable machine learning and impact of uncertainties. *Geoscientific Model Development*, **15**, 4331–4354, https://doi.org/10.5194/gmd-15-4331-2022.

Bhartia, P. K., R. D. McPeters, L. E. Flynn, S. Taylor, N. A. Kramarova, S. Frith, B. Fisher, and M. DeLand, 2013: Solar Backscatter UV (SBUV) total ozone and profile algorithm. *Atmospheric Measurement Techniques*, **6**, 2533–2548, https://doi.org/10.5194/amt-6-2533-2013.

Bockarie, A. S., E. A. Marais, and A. R. MacKenzie, 2020: Air pollution and climate forcing of the charcoal industry in Africa. *Environmental Science & Technology*, **54**, 13 429–13 438, https://doi.org/10.1021/acs.est.0c03754.

Bocquet, M., and Coauthors, 2015: Data assimilation in atmospheric chemistry models: current status and future prospects for coupled chemistry meteorology models. *Atmospheric Chemistry and Physics*, **15 (10)**, 5325–5358, https://doi.org/10.5194/acp-15-5325-2015.

Bovensmann, H., J. P. Burrows, M. Buchwitz, J. Frerick, S. Noël, V. V. Rozanov, K. V. Chance, and A. P. H. Goede, 1999: SCIAMACHY: Mission objectives and measurement modes. *Journal of the Atmospheric Sciences*, **56 (2)**, 127 – 150, https://doi.org/10.1175/1520-0469(1999)056⟨0127:SMOAMM⟩2.0.CO;2, URL https://journals.ametsoc.org/view/journals/atsc/56/2/1520-0469_1999_056_0127_smoamm_2.0.co_2.xml.

Brasseur, G., and C. Granier, 2020: Use of geostationary satellites to improve air quality characterization and forecasts. https://www.issibern.ch/scientific-opportunities/international-teams/.

Buchholz, R. R., and Coauthors, 2021: Air pollution trends measured from Terra: CO and AOD over industrial fire-prone and background regions. *Remote Sensing of Environment*, **256**, 112 275, https://doi.org/10.1016/j.rse.2020.112275.

Burrows, J. P., and Coauthors, 1999: The Global Ozone Monitoring Experiment (GOME): Mission concept and first scientific results. *Journal of the Atmospheric Sciences*, **56**, 151–175, https://doi.org/10.1175/1520-0469(1999)056⟨0151:TGOMEG⟩2.0.CO;2.

Cao, H., and Coauthors, 2018: Adjoint inversion of chinese non-methane volatile organic compound emissions using space-based observations of formaldehyde and glyoxal. *Atmospheric Chemistry and Physics*, **18**, 15 017–15 046, https://doi.org/10.5194/acp-18-15017-2018.

Carmichael, G. R., A. Sandu, T. Chai, D. N. Daescu, E. M. Constantinescu, and Y. Tang, 2008: Predicting air quality: Improvements through advanced methods to integrate models and measurements. *Journal of Computational Physics*, **227**, 3540–3571, https://doi.org/10.1016/j.jcp.2007.02.024.

Carr, J., X. Liu, B. Baker, and K. Chance, 2017: Observing nightlights from space with TEMPO. *International Journal of Sustainable Lighting*, **19**, 26–35, https://doi.org/10.26607/ijsl.v19i1.64.

CEOS, 2019: Geostationary satellite constellation for observing global air quality: Geophysical validation needs. Tech. rep., CEOS Atmospheric Composition Virtual Constellation and the CEOS Working Group on Calibration and Validation. URL https://ceos.org/observations/documents/GEO_AQ_Constellation_Geophysical_Validation_Needs_1.1_2Oct2019.pdf.

Chan, K. L., E. Khorsandi, S. Liu, F. Baier, and P. Valks, 2021: Estimation of surface NO_2 concentrations over germany from TROPOMI satellite observations using a machine learning method. *Remote Sensing*, **13**, 969, https://doi.org/10.3390/rs13050969.

Chen, B., J. Hu, and Y. Wang, 2024: Synergistic observation of FY-4A&4B to estimate CO concentration in china: combining interpretable machine learning to reveal the influencing mechanisms of co variations. *npj Climate and Atmospheric Science*, **7**, 9, https://doi.org/10.1038/s41612-023-00559-0.

Chen, X., and Coauthors, 2021a: First retrieval of absorbing aerosol height over dark target using TROPOMI oxygen B band: Algorithm development and application for surface particulate matter estimates. *Remote Sensing of Environment*, **265**, 112 674, https://doi.org/https://doi.org/10.1016/j.rse.2021.112674, URL https://www.sciencedirect.com/science/article/pii/S0034425721003941.

Chen, Y., and Coauthors, 2021b: High-resolution hybrid inversion of IASI ammonia columns to constrain US ammonia emissions using the CMAQ adjoint model. *Atmospheric Chemistry and Physics*, **21**, 2067–2082, https://doi.org/10.5194/acp-21-2067-2021.

Cho, Y., and Coauthors, 2023: First atmospheric aerosol monitoring results from Geostationary Environment Monitoring Spectrometer (GEMS) over Asia. *Atmospheric Measurement Techniques Discussions*, **2023**, 1–29, https://doi.org/10.5194/amt-2023-221, URL https://amt.copernicus.org/preprints/amt-2023-221/.

Clarisse, L., Y. R'Honi, P.-F. Coheur, D. Hurtmans, and C. Clerbaux, 2011: Thermal infrared nadir observations of 24 atmospheric gases. *Geophysical Research Letters*, **38**, n/a–n/a, https://doi.org/10.1029/2011GL047271.

Clarisse, L., M. Van Damme, C. Clerbaux, and P.-F. Coheur, 2019: Tracking down global NH_3 point sources with wind-adjusted superresolution. *Atmospheric Measurement Techniques*, **12 (10)**, 5457–5473, https://doi.org/10.5194/amt-12-5457-2019, URL https://amt.copernicus.org/articles/12/5457/2019/.

Clarisse, L., M. Van Damme, D. Hurtmans, B. Franco, C. Clerbaux, and P.-F. Coheur, 2021: The diel cycle of NH_3 observed from the FY-4A Geostationary Interferometric Infrared Sounder (GIIRS). *Geophysical Research Letters*, **48 (14)**, e2021GL093 010, https://doi.org/https://doi.org/10.1029/2021GL093010, URL https://agupubs.onlinelibrary.wiley.com/doi/abs/10.1029/2021GL093010, e2021GL093010 2021GL093010, https://agupubs.onlinelibrary.wiley.com/doi/pdf/10.1029/2021GL093010.

Clarisse, L., and Coauthors, 2023: The IASI NH_3 version 4 product: averaging kernels and improved consistency. *Atmospheric Measurement Techniques*, **16**, 5009–5028, https://doi.org/10.5194/amt-16-5009-2023.

Clerbaux, C., and C. Crevoisier, 2013: New directions: Infrared remote sensing of the troposphere from satellite: Less, but better. *Atmospheric Environment*, **72**, 24–26, https://doi.org/10.1016/j.atmosenv.2013.01.057.

Clerbaux, C., and Coauthors, 2009: Monitoring of atmospheric composition using the thermal infrared IASI/MetOp sounder. *Atmospheric Chemistry and Physics*, **9 (16)**, 6041–6054, https://doi.org/10.5194/acp-9-6041-2009.

Cohen, A. J., and Coauthors, 2017: Estimates and 25-year trends of the global burden of disease attributable to ambient air pollution: an analysis of data from the global burden of diseases study 2015. *The Lancet*, **389**, 1907–1918, https://doi.org/10.1016/S0140-6736(17)30505-6.

Cooper, M., R. V. Martin, A. Padmanabhan, and D. K. Henze, 2017: Comparing mass balance and adjoint methods for inverse modeling of nitrogen dioxide columns for global nitrogen oxide emissions. *Journal of Geophysical Research: Atmospheres*, **122**, 4718–4734, https://doi.org/10.1002/2016JD025985.

Coopmann, O., N. Fourrié, P. Chambon, J. Vidot, P. Brousseau, M. Martet, and C. Birman, 2023: Preparing the assimilation of the future MTG-IRS sounder into the mesoscale numerical weather prediction AROME model. *Quarterly Journal of the Royal Meteorological Society*, **149**, 3110–3134, https://doi.org/10.1002/qj.4548.

Crevoisier, C., and Coauthors, 2014: Towards IASI-New Generation (IASI-NG): impact of improved spectral resolution and radiometric noise on the retrieval of thermodynamic, chemistry and climate variables. *Atmospheric Measurement Techniques*, **7**, 4367–4385, https://doi.org/10.5194/amt-7-4367-2014.

Crippa, M., and Coauthors, 2023a: *GHG emissions of all world countries*. JRC134504, Publications Office of the European Union, Luxembourg, https://doi.org/10.2760/953322.

Crippa, M., and Coauthors, 2023b: The HTAP_v3 emission mosaic: merging regional and global monthly emissions (2000–2018) to support air quality modelling and policies. *Earth System Science Data*, **15**, 2667–2694, https://doi.org/10.5194/essd-15-2667-2023.

Crippa, M., and Coauthors, 2024: EDGAR v8.1 Global Air Pollutant Emissions. European Commission, Joint Research Centre (JRC), URL http://data.europa.eu/89h/a3af16e4-21ac-420a-b98c-b78a9b7723be, [Dataset].

Dai, T., Y. Cheng, D. Goto, Y. Li, X. Tang, G. Shi, and T. Nakajima, 2021: Revealing the sulfur dioxide emission reductions in China by assimilating surface observations in WRF-Chem. *Atmospheric Chemistry and Physics*, **21**, 4357–4379, https://doi.org/10.5194/acp-21-4357-2021.

Damme, M. V., L. Clarisse, T. Stavrakou, R. W. Kruit, L. Sellekaerts, C. Viatte, C. Clerbaux, and P.-F. Coheur, 2022: On the weekly cycle of atmospheric ammonia over European agricultural hotspots. *Scientific Reports*, **12**, 12 327, https://doi.org/10.1038/s41598-022-15836-w.

Dechezleprêtre, A., N. Rivers, and B. Stadler, 2019: The economic cost of air pollution: Evidence from Europe. **(1584)**, https://doi.org/https://doi.org/https://doi.org/10.1787/56119490-en, URL https://www.oecd-ilibrary.org/content/paper/56119490-en.

Di, Q., and Coauthors, 2019: An ensemble-based model of PM2.5 concentration across the contiguous United States with high spatiotemporal resolution. *Environment International*, **130**, 104 909, https://doi.org/10.1016/j.envint.2019.104909.

Di, Q., and Coauthors, 2020: Assessing NO_2 concentration and model uncertainty with high spatiotemporal resolution across the contiguous United States using ensemble model averaging. *Environmental Science & Technology*, **54**, 1372–1384, https://doi.org/10.1021/acs.est.9b03358.

Ding, J., R. van der A, B. Mijling, J. de Laat, H. Eskes, and K. F. Boersma, 2022: NO_x emissions in India derived from OMI satellite observations. *Atmospheric Environment: X*, **14**, 100 174, https://doi.org/10.1016/j.aeaoa.2022.100174.

Ding, J., R. J. van der A, H. J. Eskes, B. Mijling, T. Stavrakou, J. H. G. M. van Geffen, and J. P. Veefkind, 2020: NO_x emissions reduction and rebound in China due to the COVID-19 crisis. *Geophysical Research Letters*, **47**, https://doi.org/10.1029/2020GL089912.

Ding, J., R. J. van der A, B. Mijling, and P. F. Levelt, 2017: Space-based NO_x emission estimates over remote regions improved in DECSO. *Atmospheric Measurement Techniques*, **10**, 925–938, https://doi.org/10.5194/amt-10-925-2017.

Douros, J., and Coauthors, 2023: Comparing Sentinel-5P TROPOMI NO_2 column observations with the CAMS regional air quality ensemble. *Geoscientific Model Development*, **16**, 509–534, https://doi.org/10.5194/gmd-16-509-2023.

Drummond, J. R., and G. S. Mand, 1996: The Measurements of Pollution in the Troposphere (MOPITT) Instrument: Overall performance and calibration requirements. *Journal of Atmospheric and Oceanic Technology*, **13 (2)**, 314–320, https://doi.org/10.1175/1520-0426(1996)013⟨0314:tmopit⟩2.0.co;2.

Drummond, J. R., Z. Vaziri Zanjani, F. Nichitiu, and J. Zou, 2022: A 20-year review of the performance and operation of the MOPITT instrument. *Advances in Space Research*, **70 (10)**, 3078–3091, https://doi.org/https://doi.org/10.1016/j.asr.2022.09.010, URL https://www.sciencedirect.com/science/article/pii/S0273117722008468.

Duncan, B. N., L. N. Lamsal, A. M. Thompson, Y. Yoshida, Z. Lu, D. G. Streets, M. M. Hurwitz, and K. E. Pickering, 2016: A space-based, high-resolution view of notable changes in urban NO_x pollution around the world (2005–2014). *Journal of Geophysical Research: Atmospheres*, **121 (2)**, 976–996, https://doi.org/https://doi.org/10.1002/2015JD024121, URL https://agupubs.onlinelibrary.wiley.com/doi/abs/10.1002/2015JD024121, https://agupubs.onlinelibrary.wiley.com/doi/pdf/10.1002/2015JD024121.

East, J. D., and Coauthors, 2022: Inferring and evaluating satellite-based constraints on NO_x emissions estimates in air quality simulations. *Atmospheric Chemistry and Physics*, **22 (24)**, 15 981–16 001, https://doi.org/10.5194/acp-22-15981-2022.

Edwards, D. P., and Coauthors, 2024: Quantifying the diurnal variation of atmospheric NO_2 from observations of the Geostationary Environment Monitoring Spectrometer (GEMS). *EGUsphere*, **2024**, 1–31, https://doi.org/10.5194/egusphere-2024-570, URL https://egusphere.copernicus.org/preprints/2024/egusphere-2024-570/.

Elbern, H., H. Schmidt, O. Talagrand, and A. Ebel, 2000: 4D-variational data assimilation with an adjoint air quality model for emission analysis. *Environmental Modelling & Software*, **15**, 539–548, https://doi.org/10.1016/S1364-8152(00)00049-9.

Elguindi, N., and Coauthors, 2020: Intercomparison of magnitudes and trends in anthropogenic surface emissions from bottom-up inventories top-down estimates and emission scenarios. *Earth's Future*, **8 (8)**, https://doi.org/10.1029/2020ef001520.

Environment and Climate Change Canada, 2019: Canada's air pollutant emissions inventory report. Environment and Climate Change Canada, URL https://publications.gc.ca/site/eng/9.869731/publication.html, iSSN 2562-4903.

Eskes, H., and Coauthors, 2024: Technical note: Evaluation of the Copernicus Atmosphere Monitoring Service Cy48R1 upgrade of June 2023. *EGUsphere*, **2024**, 1–57, https://doi.org/10.5194/egusphere-2023-3129, URL https://egusphere.copernicus.org/preprints/2024/egusphere-2023-3129/.

Eskes, H. J., and K. F. Boersma, 2003: Averaging kernels for doas total-column satellite retrievals. *Atmospheric Chemistry and Physics*, **3**, 1285–1291, https://doi.org/10.5194/acp-3-1285-2003.

European Environment Agency, 2023: *EMEP/EEA Air Pollutant Emission Inventory Guidebook 2023: Technical Guidance to Prepare National Emission Inventories*. European Environment Agency, https://doi.org/10.2800/795737.

Feng, S., F. Jiang, Z. Wu, H. Wang, W. Ju, and H. Wang, 2020: CO emissions inferred from surface CO observations over China in December 2013 and 2017. *Journal of Geophysical Research: Atmospheres10.1016/j.rse.2020.111644*, **125 (7)**, https://doi.org/10.1029/2019jd031808.

Fioletov, V., C. A. McLinden, D. Griffin, N. Theys, D. G. Loyola, P. Hedelt, N. A. Krotkov, and C. Li, 2020: Anthropogenic and volcanic point source SO_2 emissions derived from TROPOMI on board Sentinel-5 Precursor: first results. *Atmospheric Chemistry and Physics*, **20 (9)**, 5591–5607, https://doi.org/10.5194/acp-20-5591-2020, URL https://acp.copernicus.org/articles/20/5591/2020/.

Fioletov, V., and Coauthors, 2017: Multi-source SO_2 emission retrievals and consistency of satellite and surface measurements with reported emissions. *Atmospheric Chemistry and Physics*, **17**, 12 597–12 616, https://doi.org/10.5194/acp-17-12597-2017.

Fioletov, V. E., C. A. McLinden, N. Krotkov, and C. Li, 2015: Lifetimes and emissions of SO_2 from point sources estimated from OMI. *Geophysical Research Letters*, **42 (6)**, 1969–1976, https://doi.org/https://doi.org/10.1002/2015GL063148, URL https://agupubs.onlinelibrary.wiley.com/doi/abs/10.1002/2015GL063148, https://agupubs.onlinelibrary.wiley.com/doi/pdf/10.1002/2015GL063148.

Fortems-Cheiney, A., and Coauthors, 2021: Variational regional inverse modeling of reactive species emissions with PYVAR-CHIMERE-v2019. *Geoscientific Model Development*, **14**, 2939–2957, https://doi.org/10.5194/gmd-14-2939-2021.

Franco, B., L. Clarisse, M. V. Damme, J. Hadji-Lazaro, C. Clerbaux, and P.-F. Coheur, 2022: Ethylene industrial emitters seen from space. *Nature Communications*, **13**, 6452, https://doi.org/10.1038/s41467-022-34098-8.

Franco, B., and Coauthors, 2018: A general framework for global retrievals of trace gases from IASI: Application to methanol, formic acid, and PAN. *Journal of Geophysical Research: Atmospheres*, **123**, https://doi.org/10.1029/2018JD029633.

Franco, B., and Coauthors, 2019: Acetone atmospheric distribution retrieved from space. *Geophysical Research Letters*, **46**, 2884–2893, https://doi.org/10.1029/2019GL082052.

Frederick, S. E., R. P. Cebula, and D. F. Heath, 1986: Instrument characterization for the detection of long-term changes in stratospheric ozone: An analysis of the SBUY/2 radiometer. *Journal of Atmospheric and Oceanic Technology*, **3 (3)**, 472 – 480, https://doi.org/10.1175/1520-0426(1986)003⟨0472:ICFTDO⟩2.0.CO;2, URL https://journals.ametsoc.org/view/journals/atot/3/3/1520-0426_1986_003_0472_icftdo_2_0_co_2.xml.

Fu, D., D. B. Millet, K. C. Wells, V. H. Payne, S. Yu, A. Guenther, and A. Eldering, 2019: Direct retrieval of isoprene from satellite-based infrared measurements. *Nature Communications*, **10 (1)**, https://doi.org/10.1038/s41467-019-11835-0.

Fu, T.-M., and Coauthors, 2007: Space-based formaldehyde measurements as constraints on volatile organic compound emissions in east and south Asia and implications for ozone. *Journal of Geophysical Research: Atmospheres*, **112 (D6)**, https://doi.org/https://doi.org/10.1029/2006JD007853, URL https://agupubs.onlinelibrary.wiley.com/doi/abs/10.1029/2006JD007853, https://agupubs.onlinelibrary.wiley.com/doi/pdf/10.1029/2006JD007853.

Gaubert, B., and Coauthors, 2017: Chemical feedback from decreasing carbon monoxide emissions. *Geophysical Research Letters*, **44 (19)**, 9985–9995, https://doi.org/10.1002/2017gl074987.

Gaubert, B., and Coauthors, 2020: Correcting model biases of CO in East Asia: impact on oxidant distributions during KORUS-AQ. *Atmospheric Chemistry and Physics*, **20 (23)**, 14 617–14 647, https://doi.org/10.5194/acp-20-14617-2020.

Gaubert, B., and Coauthors, 2023: Global scale inversions from MOPITT CO and MODIS AOD. *Remote Sensing*, **15 (19)**, 4813, https://doi.org/10.3390/rs15194813.

Ghahremanloo, M., Y. Lops, Y. Choi, and B. Yeganeh, 2021: Deep learning estimation of daily ground-level NO_2 concentrations from remote sensing data. *Journal of Geophysical Research: Atmospheres*, **126**, https://doi.org/10.1029/2021JD034925.

Gkatzelis, G. I., and Coauthors, 2021: The global impacts of COVID-19 lockdowns on urban air pollution. *Elementa: Science of the Anthropocene*, **9**, https://doi.org/10.1525/elementa.2021.00176.

Goris, N., and H. Elbern, 2013: Singular vector decomposition for sensitivity analyses of tropospheric chemical scenarios. *Atmospheric Chemistry and Physics*, **13 (9)**, 5063–5087, https://doi.org/10.5194/acp-13-5063-2013.

Government of Canada, 2018: Government of Canada's Greenhouse Gas Emissions Inventory. Treasury Board of Canada Secretariat, URL https://publications.gc.ca/site/eng/9.849459/publication.html, iSSN 2562-2927.

Granier, C., C. Liousse, B. McDonald, and P. Middleton, 2023: *Anthropogenic Emissions Inventories of Air Pollutants*, 3–52. Springer Nature Singapore, Singapore, https://doi.org/10.1007/978-981-15-2760-9_5, URL https://doi.org/10.1007/978-981-15-2760-9_5.

Guanter, L., and Coauthors, 2021: The TROPOSIF global sun-induced fluorescence dataset from the Sentinel-5P TROPOMI mission. *Earth System Science Data*, **13 (11)**, 5423–5440, https://doi.org/10.5194/essd-13-5423-2021.

Guevara, M., and Coauthors, 2021: Copernicus Atmosphere Monitoring Service TEMPOral profiles (CAMS-TEMPO): global and European emission temporal profile maps for atmospheric chemistry modelling. *Earth System Science Data*, **13 (2)**, 367–404, https://doi.org/10.5194/essd-13-367-2021.

Ha, E. S., and Coauthors, 2024: First evaluation of the GEMS glyoxal products against TROPOMI and ground-based measurements. *EGUsphere*, **2024**, 1–25, https://doi.org/10.5194/egusphere-2024-589, URL https://egusphere.copernicus.org/preprints/2024/egusphere-2024-589/.

Han, S., W. Kundhikanjana, P. Towashiraporn, and D. Stratoulias, 2022: Interpolation-based fusion of Sentinel-5P, SRTM, and regulatory-grade ground stations data for producing spatially continuous maps of PM2.5 concentrations nationwide over Thailand. *Atmosphere*, **13**, 161, https://doi.org/10.3390/atmos13020161.

Han, Y., and Coauthors, 2013: Suomi NPP CrIS measurements, sensor data record algorithm, calibration and validation activities, and record data quality. *Journal of Geophysical Research: Atmospheres*, **118**, https://doi.org/10.1002/2013JD020344.

He, T.-L., R. J. Boyd, D. J. Varon, and A. J. Turner, 2024a: Increased methane emissions from oil and gas following the Soviet Union's collapse. *Proceedings of the National Academy of Sciences*, **121 (12)**, e2314600 121, https://doi.org/10.1073/pnas.2314600121, URL https://www.pnas.org/doi/abs/10.1073/pnas.2314600121, https://www.pnas.org/doi/pdf/10.1073/pnas.2314600121.

He, T.-L., N. Dadheech, T. Thompson, and A. Turner, 2024b: FootNet v1.0: Development of a machine learning emulator of atmospheric transport. *EarthArXiv*, https://doi.org/10.31223/x5197g, URL http://dx.doi.org/10.31223/X5197G.

He, T.-L., and Coauthors, 2022a: Deep learning to evaluate US NO_x emissions using surface ozone predictions. *Journal of Geophysical Research: Atmospheres*, **127 (4)**, e2021JD035 597, https://doi.org/https://doi.org/10.1029/2021JD035597, URL https://agupubs.onlinelibrary.wiley.com/doi/abs/10.1029/2021JD035597, e2021JD035597 2021JD035597, https://agupubs.onlinelibrary.wiley.com/doi/pdf/10.1029/2021JD035597.

He, T.-L., and Coauthors, 2022b: Inverse modelling of Chinese NO_x emissions using deep learning: integrating in situ observations with a satellite-based chemical reanalysis. *Atmospheric Chemistry and Physics*, **22 (21)**, 14 059–14 074, https://doi.org/10.5194/acp-22-14059-2022.

Heath, D. F., A. J. Krueger, H. A. Roeder, and B. D. Henderson, 1975: The Solar Backscatter Ultraviolet and Total Ozone Mapping Spectrometer (SBUV/TOMS) for NIMBUS G. *Optical Engineering*, **14 (4)**, 144 323, https://doi.org/10.1117/12.7971839, URL https://doi.org/10.1117/12.7971839.

Hedelius, J. K., and Coauthors, 2021: Regional and urban column CO trends and anomalies as observed by MOPITT over 16 years. *Journal of Geophysical Research: Atmospheres*, **126 (5)**, https://doi.org/10.1029/2020jd033967.

Henze, D. K., A. Hakami, and J. H. Seinfeld, 2007: Development of the adjoint of GEOS-Chem. *Atmospheric Chemistry and Physics*, **7**, 2413–2433, https://doi.org/10.5194/acp-7-2413-2007.

Heue, K.-P., D. Loyola, F. Romahn, W. Zimmer, S. Chabrillat, Q. Errera, J. Ziemke, and N. Kramarova, 2022: Tropospheric ozone retrieval by a combination of TROPOMI/S5P measurements with BASCOE assimilated data. *Atmospheric Measurement Techniques*, **15**, 5563–5579, https://doi.org/10.5194/amt-15-5563-2022.

Hickman, J. E., and Coauthors, 2021: Changes in biomass burning wetland extent or agriculture drive atmospheric NH_3 trends in select African regions. *Atmospheric Chemistry and Physics*, **21 (21)**, 16 277–16 291, https://doi.org/10.5194/acp-21-16277-2021.

Huang, L., and Coauthors, 2021: Exploring deep learning for air pollutant emission estimation. *Geoscientific Model Development*, **14 (7)**, 4641–4654, https://doi.org/10.5194/gmd-14-4641-2021, URL https://gmd.copernicus.org/articles/14/4641/2021/.

Huang, X., Z. Deng, F. Jiang, M. Zhou, X. Lin, Z. Liu, and M. Peng, 2024: Improved consistency of satellite XCO_2 retrievals based on machine learning. *Geophysical Research Letters*, **51 (8)**, e2023GL107 536, https://doi.org/https://doi.org/10.1029/2023GL107536, URL https://agupubs.onlinelibrary.wiley.com/doi/abs/10.1029/2023GL107536, e2023GL107536 2023GL107536, https://agupubs.onlinelibrary.wiley.com/doi/pdf/10.1029/2023GL107536.

Hyman, D. M., and M. J. Pavolonis, 2020: Probabilistic retrieval of volcanic SO_2 layer height and partial column density using the Cross-track Infrared Sounder (CrIS). *Atmospheric Measurement Techniques*, **13 (11)**, 5891–5921, https://doi.org/10.5194/amt-13-5891-2020, URL https://amt.copernicus.org/articles/13/5891/2020/.

Inness, A., and Coauthors, 2015: Data assimilation of satellite-retrieved ozone carbon monoxide and nitrogen dioxide with ECMWF's Composition-IFS. *Atmospheric Chemistry and Physics*, **15 (9)**, 5275–5303, https://doi.org/10.5194/acp-15-5275-2015.

Inness, A., and Coauthors, 2019: The CAMS reanalysis of atmospheric composition. *Atmospheric Chemistry and Physics*, **19 (6)**, 3515–3556, https://doi.org/10.5194/acp-19-3515-2019.

Inness, A., and Coauthors, 2022: Assimilation of S5P/TROPOMI carbon monoxide data with the global CAMS near-real-time system. *Atmospheric Chemistry and Physics*, **22 (21)**, 14 355–14 376, https://doi.org/10.5194/acp-22-14355-2022.

Jiang, Z., and Coauthors, 2018: Unexpected slowdown of US pollutant emission reduction in the past decade. *Proceedings of the National Academy of Sciences*, **115 (20)**, 5099–5104, https://doi.org/10.1073/pnas.1801191115.

Jiang, Z., and Coauthors, 2022: Decadal variabilities in tropospheric nitrogen oxides over United States, Europe, and China. *Journal of Geophysical Research: Atmospheres*, **127**, https://doi.org/10.1029/2021JD035872.

Kalnay, E., H. Li, T. Miyoshi, S.-C. Yang, and J. Ballabrera-Poy, 2007: 4-D-Var or ensemble Kalman filter? *Tellus A: Dynamic Meteorology and Oceanography*, **59**, 758, https://doi.org/10.1111/j.1600-0870.2007.00261.x.

Keita, S., and Coauthors, 2021: African anthropogenic emissions inventory for gases and particles from 1990 to 2015. *Earth System Science Data*, **13 (7)**, 3691–3705, https://doi.org/10.5194/essd-13-3691-2021, URL https://essd.copernicus.org/articles/13/3691/2021/.

Keller, C. A., and M. J. Evans, 2019: Application of random forest regression to the calculation of gas-phase chemistry within the GEOS-Chem chemistry model v10. *Geoscientific Model Development*, **12**, 1209–1225, https://doi.org/10.5194/gmd-12-1209-2019.

Kelp, M. M., D. J. Jacob, J. N. Kutz, J. D. Marshall, and C. W. Tessum, 2020: Toward stable, general machine-learned models of the atmospheric chemical system. *Journal of Geophysical Research: Atmospheres*, **125**, https://doi.org/10.1029/2020JD032759.

Kelp, M. M., D. J. Jacob, H. Lin, and M. P. Sulprizio, 2022: An online-learned neural network chemical solver for stable long-term global simulations of atmospheric chemistry. *Journal of Advances in Modeling Earth Systems*, **14**, https://doi.org/10.1029/2021MS002926.

Kim, J., and Coauthors, 2020: New era of air quality monitoring from space: Geostationary Environment Monitoring Spectrometer (GEMS). *Bulletin of the American Meteorological Society*, **101 (1)**, E1 – E22, https://doi.org/10.1175/BAMS-D-18-0013.1, URL https://journals.ametsoc.org/view/journals/bams/101/1/bams-d-18-0013.1.xml.

Kim, S., and Coauthors, 2023: First-time comparison between NO_2 vertical columns from Geostationary Environmental Monitoring Spectrometer (GEMS) and Pandora measurements. *Atmospheric Measurement Techniques*, **16**, 3959–3972, https://doi.org/10.5194/amt-16-3959-2023.

Kim, Y., Y. Wu, C. Seigneur, and Y. Roustan, 2018: Multi-scale modeling of urban air pollution: development and application of a Street-in-Grid model (v1.0) by coupling MUNICH (v1.0) and Polair3D (v1.8.1). *Geoscientific Model Development*, **11**, 611–629, https://doi.org/10.5194/gmd-11-611-2018.

Klimont, Z., K. Kupiainen, C. Heyes, P. Purohit, J. Cofala, P. Rafaj, J. Borken-Kleefeld, and W. Schöpp, 2017: Global anthropogenic emissions of particulate matter including black carbon. *Atmospheric Chemistry and Physics*, **17 (14)**, 8681–8723, https://doi.org/10.5194/acp-17-8681-2017, URL https://acp.copernicus.org/articles/17/8681/2017/.

Kong, H., and Coauthors, 2019: High-resolution ($0.05° \times 0.05°$) NO_x emissions in the Yangtze River Delta inferred from OMI. *Atmospheric Chemistry and Physics*, **19**, 12 835–12 856, https://doi.org/10.5194/acp-19-12835-2019.

Kong, H., and Coauthors, 2022: Considerable unaccounted local sources of NO_x emissions in China revealed from satellite. *Environmental Science & Technology*, **56**, 7131–7142, https://doi.org/10.1021/acs.est.1c07723.

Krol, M., B. van Stratum, I. Anglou, and K. F. Boersma, 2024: Estimating NO_x emissions of stack plumes using a high-resolution atmospheric chemistry model and satellite-derived NO_2 columns. *EGUsphere*, **2024**, 1–32, https://doi.org/10.5194/egusphere-2023-2519, URL https://egusphere.copernicus.org/preprints/2024/egusphere-2023-2519/.

Kuenen, J., S. Dellaert, A. Visschedijk, J.-P. Jalkanen, I. Super, and H. Denier van der Gon, 2021: Copernicus Atmosphere Monitoring Service regional emissions version 5.1 business-as-usual 2020 (CAMS-REG-v5.1 BAU 2020). Copernicus Atmosphere Monitoring Service, eCCAD [distributor], https://doi.org/10.24380/eptm-kn40.

Kurokawa, J., and T. Ohara, 2020: Long-term historical trends in air pollutant emissions in Asia: Regional Emission inventory in ASia (REAS) version 3. *Atmospheric Chemistry and Physics*, **20 (21)**, 12 761–12 793, https://doi.org/10.5194/acp-20-12761-2020, URL https://acp.copernicus.org/articles/20/12761/2020/.

Kurokawa, J.-i., K. Yumimoto, I. Uno, and T. Ohara, 2009: Adjoint inverse modeling of NO_x emissions over eastern China using satellite observations of NO_2 vertical column densities. *Atmospheric Environment*, **43 (11)**, 1878–1887, https://doi.org/10.1016/j.atmosenv.2008.12.030.

Lahoz, W. A., and P. Schneider, 2014: Data assimilation: making sense of Earth Observation. *Frontiers in Environmental Science*, **2**, https://doi.org/10.3389/fenvs.2014.00016.

Lambrigtsen, B., E. Fetzer, E. Fishbein, S.-Y. Lee, and T. Pagano, 2004: AIRS - the Atmospheric Infrared Sounder. *IGARSS 2004. 2004 IEEE International Geoscience and Remote Sensing Symposium*, Vol. 3, 2204–2207 vol.3, https://doi.org/10.1109/IGARSS.2004.1370798.

Lamsal, L. N., B. N. Duncan, Y. Yoshida, N. A. Krotkov, K. E. Pickering, D. G. Streets, and Z. Lu, 2015: U.S. NO_2 trends (2005–2013): EPA Air Quality System (AQS) data versus improved observations from the Ozone Monitoring Instrument (OMI). *Atmospheric Environment*, **110**, 130–143, https://doi.org/https://doi.org/10.1016/j.atmosenv.2015.03.055, URL https://www.sciencedirect.com/science/article/pii/S1352231015002794.

Lamsal, L. N., and Coauthors, 2021: Ozone Monitoring Instrument (OMI) Aura nitrogen dioxide standard product version 4.0 with improved surface and cloud treatments. *Atmospheric Measurement Techniques*, **14**, 455–479, https://doi.org/10.5194/amt-14-455-2021.

Lange, K., and Coauthors, 2024: Validation of GEMS tropospheric NO_2 columns and their diurnal variation with ground-based DOAS measurements. *Atmospheric Measurement Techniques*, **17 (21)**, 6315–6344, https://doi.org/10.5194/amt-17-6315-2024, URL https://amt.copernicus.org/articles/17/6315/2024/.

Lee, G. T., and Coauthors, 2024: First evaluation of the GEMS formaldehyde product against TROPOMI and ground-based column measurements during the in-orbit test period. *Atmospheric Chemistry and Physics*, **24**, 4733–4749, https://doi.org/10.5194/acp-24-4733-2024.

Lerot, C., and Coauthors, 2021: Glyoxal tropospheric column retrievals from TROPOMI – multi-satellite intercomparison and ground-based validation. *Atmospheric Measurement Techniques*, **14**, 7775–7807, https://doi.org/10.5194/amt-14-7775-2021.

Levelt, P. F., and Coauthors, 2018: The Ozone Monitoring Instrument: overview of 14 years in space. *Atmospheric Chemistry and Physics*, **18 (8)**, 5699–5745, https://doi.org/10.5194/acp-18-5699-2018.

Li, L., and Coauthors, 2023a: Improving air quality assessment using physics-inspired deep graph learning. *npj Climate and Atmospheric Science*, **6 (1)**, 152, https://doi.org/10.1038/s41612-023-00475-3, URL https://doi.org/10.1038/s41612-023-00475-3.

Li, M., and Coauthors, 2023b: MIXv2: a long-term mosaic emission inventory for Asia (2010–2017). *EGUsphere*, **2023**, 1–45, https://doi.org/10.5194/egusphere-2023-2283, URL https://egusphere.copernicus.org/preprints/2023/egusphere-2023-2283/.

Li, R., and Coauthors, 2022: Representation of leaf-to-canopy radiative transfer processes improves simulation of far-red solar-induced chlorophyll fluorescence in the Community Land Model Version 5. *Journal of Advances in Modeling Earth Systems*, **14 (3)**, https://doi.org/10.1029/2021ms002747.

Li, X., and J. Xiao, 2019: A global 0.05-degree product of solar-induced chlorophyll fluorescence derived from OCO-2 MODIS and reanalysis data. *Remote Sensing*, **11 (5)**, 517, https://doi.org/10.3390/rs11050517.

Lindsey, D. T., and Coauthors, 2024: GeoXO: NOAA's Future Geostationary Satellite System. *Bulletin of the American Meteorological Society*, **105**, E660–E679, https://doi.org/10.1175/BAMS-D-23-0048.1.

Liu, F., and Coauthors, 2020a: Abrupt decline in tropospheric nitrogen dioxide over China after the outbreak of COVID-19. *Science Advances*, **6 (28)**, eabc2992, https://doi.org/10.1126/sciadv.abc2992, URL https://www.science.org/doi/abs/10.1126/sciadv.abc2992, https://www.science.org/doi/pdf/10.1126/sciadv.abc2992.

Liu, T., L. J. Mickley, M. E. Marlier, R. S. DeFries, M. F. Khan, M. T. Latif, and A. Karambelas, 2020b: Diagnosing spatial biases and uncertainties in global fire emissions inventories: Indonesia as regional case study. *Remote Sensing of Environment*, **237**, 111 557, https://doi.org/10.1016/j.rse.2019.111557.

Liu, X., A. P. Mizzi, J. L. Anderson, I. Fung, and R. C. Cohen, 2021: The potential for geostationary remote sensing of NO_2 to improve weather prediction. *Atmospheric Chemistry and Physics*, **21**, 9573–9583, https://doi.org/10.5194/acp-21-9573-2021.

Lu, X., and Coauthors, 2021: Global methane budget and trend, 2010–2017: complementarity of inverse analyses using in situ (GLOBALVIEWplus CH_4 ObsPack) and satellite (GOSAT) observations. *Atmospheric Chemistry and Physics*, **21**, 4637–4657, https://doi.org/10.5194/acp-21-4637-2021.

Ludewig, A., and Coauthors, 2020: In-flight calibration results of the TROPOMI payload on board the Sentinel-5 Precursor satellite. *Atmospheric Measurement Techniques*, **13**, 3561–3580, https://doi.org/10.5194/amt-13-3561-2020.

Luo, M., H. M. Worden, R. D. Field, K. Tsigaridis, and G. S. Elsaesser, 2024: TROPESS-CrIS CO single-pixel vertical profiles: intercomparisons with MOPITT and model simulations for 2020 western US wildfires. *Atmospheric Measurement Techniques*, **17 (9)**, 2611–2624, https://doi.org/10.5194/amt-17-2611-2024, URL https://amt.copernicus.org/articles/17/2611/2024/.

Ma, L., D. J. Graham, and M. E. J. Stettler, 2023: Using explainable machine learning to interpret the effects of policies on air pollution: COVID-19 lockdown in London. *Environmental Science & Technology*, **57 (46)**, 18 271–18 281, https://doi.org/10.1021/acs.est.2c09596, URL https://doi.org/10.1021/acs.est.2c09596, pMID: 37566731, https://doi.org/10.1021/acs.est.2c09596.

Marais, E., and K. Chance, 2015: A geostationary air quality monitoring platform for Africa. *Clean Air Journal*, **25 (1)**, 40, https://doi.org/10.17159/2410-972X/2015/v25n1a3, URL https://cleanairjournal.org.za/article/view/6925.

Marais, E. A., and C. Wiedinmyer, 2016: Air quality impact of diffuse and inefficient combustion emissions in Africa (DICE-Africa). *Environmental Science & Technology*, **50**, 10 739–10 745, https://doi.org/10.1021/acs.est.6b02602.

Marais, E. A., and Coauthors, 2012: Isoprene emissions in Africa inferred from OMI observations of formaldehyde columns. *Atmospheric Chemistry and Physics*, **12 (14)**, 6219–6235, https://doi.org/10.5194/acp-12-6219-2012.

Marais, E. A., and Coauthors, 2021: New observations of NO_2 in the upper troposphere from TROPOMI. *Atmospheric Measurement Techniques*, **14**, 2389–2408, https://doi.org/10.5194/amt-14-2389-2021.

Martínez-Alonso, S., and Coauthors, 2023: S-5P/TROPOMI-derived NO_2 emissions from copper/cobalt mining and other industrial activities in the copperbelt (Democratic Republic of Congo and Zambia). *Geophysical Research Letters*, **50 (19)**, https://doi.org/10.1029/2023gl104109.

Mateer, C. L., D. F. Heath, and A. J. Krueger, 1971: Estimation of total ozone from satellite measurements of backscattered ultraviolet earth radiance. *Journal of Atmospheric Sciences*, **28 (7)**, 1307 – 1311, https://doi.org/10.1175/1520-0469(1971)028⟨1307:EOTOFS⟩2.0.CO;2, URL https://journals.ametsoc.org/view/journals/atsc/28/7/1520-0469_1971_028_1307_eotofs_2_0_co_2.xml.

Millet, D. B., D. J. Jacob, K. F. Boersma, T.-M. Fu, T. P. Kurosu, K. Chance, C. L. Heald, and A. Guenther, 2008: Spatial distribution of isoprene emissions from North America derived from formaldehyde column measurements by the OMI satellite sensor. *Journal of Geophysical Research*, **113 (D2)**, https://doi.org/10.1029/2007jd008950.

Miyazaki, K., and K. Bowman, 2023: Predictability of fossil fuel CO_2 from air quality emissions. *Nature Communications*, **14**, 1604, https://doi.org/10.1038/s41467-023-37264-8.

Miyazaki, K., K. W. Bowman, K. Yumimoto, T. Walker, and K. Sudo, 2020a: Evaluation of a multi-model multi-constituent assimilation framework for tropospheric chemical reanalysis. *Atmospheric Chemistry and Physics*, **20 (2)**, 931–967, https://doi.org/10.5194/acp-20-931-2020.

Miyazaki, K., H. Eskes, K. Sudo, K. F. Boersma, K. Bowman, and Y. Kanaya, 2017: Decadal changes in global surface NO_x emissions from multi-constituent satellite data assimilation. *Atmospheric Chemistry and Physics*, **17 (2)**, 807–837, https://doi.org/10.5194/acp-17-807-2017.

Miyazaki, K., H. J. Eskes, and K. Sudo, 2015: A tropospheric chemistry reanalysis for the years 2005–2012 based on an assimilation of OMI MLS TES and MOPITT satellite data. *Atmospheric Chemistry and Physics*, **15 (14)**, 8315–8348, https://doi.org/10.5194/acp-15-8315-2015.

Miyazaki, K., H. J. Eskes, K. Sudo, M. Takigawa, M. van Weele, and K. F. Boersma, 2012: Simultaneous assimilation of satellite NO_2, O_3, CO, and HNO_3 data for the analysis of tropospheric chemical composition and emissions. *Atmospheric Chemistry and Physics*, **12 (20)**, 9545–9579, https://doi.org/10.5194/acp-12-9545-2012.

Miyazaki, K., J. L. Neu, G. Osterman, and K. Bowman, 2022: Changes in US background ozone associated with the 2011 turnaround in Chinese NO_x emissions. *Environmental Research Communications*, **4**, 045 003, https://doi.org/10.1088/2515-7620/ac619b.

Miyazaki, K., and Coauthors, 2020b: Updated tropospheric chemistry reanalysis and emission estimates, TCR-2, for 2005-2018. *Earth System Science Data*, **12 (3)**, 2223–2259, https://doi.org/10.5194/essd-12-2223-2020.

Munro, R., and Coauthors, 2016: The GOME-2 instrument on the Metop series of satellites: instrument design, calibration, and level 1 data processing – an overview. *Atmospheric Measurement Techniques*, **9 (3)**, 1279–1301, https://doi.org/10.5194/amt-9-1279-2016, URL https://amt.copernicus.org/articles/9/1279/2016/.

Müller, J., T. Stavrakou, M. Bauwens, M. George, D. Hurtmans, P. Coheur, C. Clerbaux, and C. Sweeney, 2018: Top-down CO emissions based on IASI observations and hemispheric constraints on OH levels. *Geophysical Research Letters*, **45**, 1621–1629, https://doi.org/10.1002/2017GL076697.

Müller, J.-F., and T. Stavrakou, 2005: Inversion of CO and NO_x emissions using the adjoint of the IMAGES model. *Atmospheric Chemistry and Physics*, **5 (5)**, 1157–1186, https://doi.org/10.5194/acp-5-1157-2005.

Müller, J.-F., and Coauthors, 2024: Bias correction of OMI HCHO columns based on FTIR and aircraft measurements and impact on top-down emission estimates. *Atmospheric Chemistry and Physics*, **24**, 2207–2237, https://doi.org/10.5194/acp-24-2207-2024.

Oak, Y. J., and Coauthors, 2024: A bias-corrected GEMS geostationary satellite product for nitrogen dioxide using machine learning to enforce consistency with the TROPOMI satellite instrument. *Atmospheric Measurement Techniques*, **17 (17)**, 5147–5159, https://doi.org/10.5194/amt-17-5147-2024, URL https://amt.copernicus.org/articles/17/5147/2024/.

O'Dell, K., S. Kondragunta, H. Zhang, D. L. Goldberg, G. H. Kerr, Z. Wei, B. H. Henderson, and S. C. Anenberg, 2024: Public health benefits from improved identification of severe air pollution events with geostationary satellite data. *GeoHealth*, **8**, https://doi.org/10.1029/2023GH000890.

Oomen, G.-M., and Coauthors, 2024: Weekly derived top-down volatile-organic-compound fluxes over Europe from TROPOMI HCHO data from 2018 to 2021. *Atmospheric Chemistry and Physics*, **24**, 449–474, https://doi.org/10.5194/acp-24-449-2024.

Park, H., and S. Jeong, 2021: Leaf area index in Earth system models: how the key variable of vegetation seasonality works in climate projections. *Environmental Research Letters*, **16 (3)**, 034 027, https://doi.org/10.1088/1748-9326/abe2cf.

Park, J., Y. Choi, J. Jung, K. Lee, and A. K. Yeganeh, 2024: First top-down diurnal adjustment to NO_x emissions inventory in Asia informed by the Geostationary Environment Monitoring Spectrometer (GEMS) tropospheric NO_2 columns. *Scientific Reports*, **14 (1)**, https://doi.org/10.1038/s41598-024-76223-1, URL http://dx.doi.org/10.1038/s41598-024-76223-1.

Park, S. S., J. Kim, Y. Cho, H. Lee, J. Park, D.-W. Lee, W.-J. Lee, and D.-R. Kim, 2023: Retrieval algorithm for aerosol effective height from the Geostationary Environment Monitoring Spectrometer (GEMS). *Atmospheric Measurement Techniques Discussions*, **2023**, 1–40, https://doi.org/10.5194/amt-2023-136, URL https://amt.copernicus.org/preprints/amt-2023-136/.

Paton-Walsh, C., and Coauthors, 2022: Key challenges for tropospheric chemistry in the southern hemisphere. *Elementa: Science of the Anthropocene*, **10**, https://doi.org/10.1525/elementa.2021.00050.

Pendergrass, D. C., and Coauthors, 2022: Continuous mapping of fine particulate matter ($PM_{2.5}$ air quality in East Asia at daily 6×6 km^2 resolution by application of a random forest algorithm to 2011–2019 GOCI geostationary satellite data. *Atmospheric Measurement Techniques*, **15**, 1075–1091, https://doi.org/10.5194/amt-15-1075-2022.

Pendergrass, D. C., and Coauthors, 2024: A continuous 2011–2022 record of fine particulate matter ($PM_{2.5}$) in East Asia at daily 2-km resolution from geostationary satellite observations: population exposure and long-term trends. *Earth System Science Data Discussions*,

2024, 1–27, https://doi.org/10.5194/essd-2024-172, URL https://essd.copernicus.org/preprints/essd-2024-172/.

Peuch, V.-H., and Coauthors, 2022: The copernicus atmosphere monitoring service: From research to operations. *Bulletin of the American Meteorological Society*, **103 (12)**, E2650–E2668, https://doi.org/10.1175/bams-d-21-0314.1.

Pfister, G. G., and Coauthors, 2020: The Multi-Scale Infrastructure for Chemistry and Aerosols (MUSICA). *Bulletin of the American Meteorological Society*, **101 (10)**, E1743–E1760, https://doi.org/10.1175/bams-d-19-0331.1.

Plauchu, R., and Coauthors, 2024: NO_x emissions in France in 2019–2021 as estimated by the high spatial resolution assimilation of TROPOMI NO_2 observations. *EGUsphere*, **2024**, 1–34, https://doi.org/10.5194/egusphere-2024-103, URL https://egusphere.copernicus.org/preprints/2024/egusphere-2024-103/.

Qu, Z., D. K. Henze, S. L. Capps, Y. Wang, X. Xu, J. Wang, and M. Keller, 2017: Monthly top-down NO_x emissions for China (2005–2012): A hybrid inversion method and trend analysis. *Journal of Geophysical Research: Atmospheres*, **122**, 4600–4625, https://doi.org/10.1002/2016JD025852.

Qu, Z., D. K. Henze, N. Theys, J. Wang, and W. Wang, 2019: Hybrid mass balance/4D-Var joint inversion of NO_x and SO_2 emissions in East Asia. *Journal of Geophysical Research: Atmospheres*, **124**, 8203–8224, https://doi.org/10.1029/2018JD030240.

Qu, Z., D. K. Henze, H. M. Worden, Z. Jiang, B. Gaubert, N. Theys, and W. Wang, 2022a: Sector-based top-down estimates of NO_x SO_2 and CO emissions in East Asia. *Geophysical Research Letters*, **49 (2)**, https://doi.org/10.1029/2021gl096009.

Qu, Z., and Coauthors, 2022b: Attribution of the 2020 surge in atmospheric methane by inverse analysis of GOSAT observations. *Environmental Research Letters*, **17 (9)**, 094 003, https://doi.org/10.1088/1748-9326/ac8754.

Riess, T. C. V. W., K. F. Boersma, J. van Vliet, W. Peters, M. Sneep, H. Eskes, and J. van Geffen, 2022: Improved monitoring of shipping NO_2 with TROPOMI: decreasing NOx emissions in European seas during the COVID-19 pandemic. *Atmospheric Mea-*

surement Techniques, **15 (5)**, 1415–1438, https://doi.org/10.5194/amt-15-1415-2022, URL https://amt.copernicus.org/articles/15/1415/2022/.

Sandu, A., and T. Chai, 2011: Chemical data assimilation-An overview. *Atmosphere*, **2 (3)**, 426–463, https://doi.org/10.3390/atmos2030426.

Savas, D., and Coauthors, 2023: Anthropogenic NOx Emission Estimations over East China for 2015 and 2019 Using OMI Satellite Observations and the New Inverse Modeling System CIF-CHIMERE. *Atmosphere*, **14**, 154, https://doi.org/10.3390/atmos14010154.

Sayeed, A., and Coauthors, 2021: A novel CMAQ-CNN hybrid model to forecast hourly surface-ozone concentrations 14 days in advance. *Scientific Reports*, **11**, 10 891, https://doi.org/10.1038/s41598-021-90446-6.

Sekiya, T., K. Miyazaki, K. Ogochi, K. Sudo, M. Takigawa, H. Eskes, and K. F. Boersma, 2021: Impacts of horizontal resolution on global data assimilation of satellite measurements for tropospheric chemistry analysis. *Journal of Advances in Modeling Earth Systems*, **13 (6)**, https://doi.org/10.1029/2020ms002180.

Shu, L., and Coauthors, 2023: Improving ozone simulations in Asia via multisource data assimilation: results from an observing system simulation experiment with GEMS geostationary satellite observations. *Atmospheric Chemistry and Physics*, **23 (6)**, 3731–3748, https://doi.org/10.5194/acp-23-3731-2023.

Silvern, R. F., and Coauthors, 2019: Using satellite observations of tropospheric NO2 columns to infer long-term trends in US NOx emissions: the importance of accounting for the free tropospheric NO2 background. *Atmospheric Chemistry and Physics*, **19 (13)**, 8863–8878, https://doi.org/10.5194/acp-19-8863-2019, URL https://acp.copernicus.org/articles/19/8863/2019/.

Sindelarova, K., S. Arellano, P. Ginoux, C. Granier, S. T. Lennartz, and D. Simpson, 2023: *Natural Emissions on Global Scale*, 53–93. Springer Nature Singapore, Singapore, https://doi.org/10.1007/978-981-15-2760-9_7, URL https://doi.org/10.1007/978-981-15-2760-9_7.

Skoulidou, I., M.-E. Koukouli, A. Segers, A. Manders, D. Balis, T. Stavrakou, J. van Geffen, and H. Eskes, 2021: Changes in power plant NOx emissions over northwest greece using a data assimilation technique. *Atmosphere*, **12**, 900, https://doi.org/10.3390/atmos12070900.

Soulie, A., and Coauthors, 2023: Global Anthropogenic Emissions (CAMS-GLOB-ANT) for the Copernicus Atmosphere Monitoring Service Simulations of Air Quality Forecasts and Reanalyses. *Earth Syst. Sci. Data Discuss.*, https://doi.org/10.5194/essd-2023-306.

Stark, H. R., H. L. Moller, G. B. Courreges-Lacoste, R. Koopman, S. Mezzasoma, and B. Veihelmann, 2013: The Sentinel-4 Mission And Its Implementation. *ESA Living Planet Symposium*, ESA Special Publication, Vol. 722, 139.

Stavrakou, T., J.-F. Müller, M. Bauwens, K. F. Boersma, and J. van Geffen, 2020: Satellite evidence for changes in the NO2 weekly cycle over large cities. *Scientific Reports*, **10 (1)**, 10 066, https://doi.org/10.1038/s41598-020-66891-0, URL https://doi.org/10.1038/s41598-020-66891-0.

Stavrakou, T., J. Müller, K. F. Boersma, I. D. Smedt, and R. J. van der A, 2008: Assessing the distribution and growth rates of NOx emission sources by inverting a 10-year record of NO_2 satellite columns. *Geophysical Research Letters*, **35**, https://doi.org/10.1029/2008GL033521.

Stavrakou, T., J.-F. Müller, M. Bauwens, I. D. Smedt, M. V. Roozendael, and A. Guenther, 2018: Impact of Short-Term Climate Variability on Volatile Organic Compounds Emissions Assessed Using OMI Satellite Formaldehyde Observations. *Geophysical Research Lettershttps://doi.org/10.1029/2003GL017336*, **45 (16)**, 8681–8689, https://doi.org/10.1029/2018gl078676.

Stavrakou, T., J.-F. Müller, K. F. Boersma, R. J. van der A, J. Kurokawa, T. Ohara, and Q. Zhang, 2013: Key chemical NO_x sink uncertainties and how they influence top-down emissions of nitrogen oxides. *Atmospheric Chemistry and Physics*, **13**, 9057–9082, https://doi.org/10.5194/acp-13-9057-2013.

Stavrakou, T., J.-F. Müller, I. D. Smedt, M. V. Roozendael, G. R. van der Werf, L. Giglio, and A. Guenther, 2009: Global emissions of non-methane hydrocarbons deduced from SCIA-

MACHY formaldehyde columns through 2003–2006. *Atmospheric Chemistry and Physics*, **9 (11)**, 3663–3679, https://doi.org/10.5194/acp-9-3663-2009.

Stavrakou, T., and Coauthors, 2012: Satellite evidence for a large source of formic acid from boreal and tropical forests. *Nature Geoscience*, **5**, 26–30, https://doi.org/10.1038/ngeo1354.

Streets, D. G., and Coauthors, 2013: Emissions estimation from satellite retrievals: A review of current capability. *Atmospheric Environment*, **77**, 1011–1042, https://doi.org/10.1016/j.atmosenv.2013.05.051.

Sun, K., and Coauthors, 2018: A physics-based approach to oversample multi-satellite, multi-species observations to a common grid. *Atmospheric Measurement Techniques*, **11 (12)**, 6679–6701, https://doi.org/10.5194/amt-11-6679-2018, URL https://amt.copernicus.org/articles/11/6679/2018/.

Tang, W., and Coauthors, 2021: Assessing sub-grid variability within satellite pixels over urban regions using airborne mapping spectrometer measurements. *Atmospheric Measurement Techniques*, **14**, 4639–4655, https://doi.org/10.5194/amt-14-4639-2021.

Tang, W., and Coauthors, 2023: Application of the multi-scale infrastructure for chemistry and aerosols version 0 (MUSICAv0) for air quality research in africa. *Geoscientific Model Development*, **16 (20)**, 6001–6028, https://doi.org/10.5194/gmd-16-6001-2023.

Tang, X., and Coauthors, 2013: Inversion of CO emissions over Beijing and its surrounding areas with ensemble Kalman filter. *Atmospheric Environment*, **81**, 676–686, https://doi.org/10.1016/j.atmosenv.2013.08.051.

Taylor, I. A., J. Preston, E. Carboni, T. A. Mather, R. G. Grainger, N. Theys, S. Hidalgo, and B. M. Kilbride, 2018: Exploring the Utility of IASI for Monitoring Volcanic SO_2 Emissions. *Journal of Geophysical Research: Atmospheres*, **123**, 5588–5606, https://doi.org/10.1002/2017JD027109.

Theys, N., and Coauthors, 2020: Global nitrous acid emissions and levels of regional oxidants enhanced by wildfires. *Nature Geoscience*, **13**, 681–686, https://doi.org/10.1038/s41561-020-0637-7.

Theys, N., and Coauthors, 2021: A sulfur dioxide Covariance-Based Retrieval Algorithm (COBRA): application to TROPOMI reveals new emission sources. *Atmospheric Chemistry and Physics*, **21**, 16 727–16 744, https://doi.org/10.5194/acp-21-16727-2021.

Tilstra, L. G., M. de Graaf, V. J. H. Trees, P. Litvinov, O. Dubovik, and P. Stammes, 2024: A directional surface reflectance climatology determined from tropomi observations. *Atmospheric Measurement Techniques*, **17**, 2235–2256, https://doi.org/10.5194/amt-17-2235-2024.

Timmermans, R., and Coauthors, 2019: Impact of synthetic space-borne NO_2 observations from the Sentinel-4 and Sentinel-5P missions on tropospheric NO_2 analyses. *Atmospheric Chemistry and Physics*, **19**, 12 811–12 833, https://doi.org/10.5194/acp-19-12811-2019.

Torres, O., P. K. Bhartia, H. Jethva, and C. Ahn, 2018: Impact of the ozone monitoring instrument row anomaly on the long-term record of aerosol products. *Atmospheric Measurement Techniques*, **11 (5)**, 2701–2715, https://doi.org/10.5194/amt-11-2701-2018.

Torres, O., H. Jethva, C. Ahn, G. Jaross, and D. G. Loyola, 2020: TROPOMI aerosol products: evaluation and observations of synoptic-scale carbonaceous aerosol plumes during 2018–2020. *Atmospheric Measurement Techniques*, **13**, 6789–6806, https://doi.org/10.5194/amt-13-6789-2020.

Valin, L. C., A. R. Russell, and R. C. Cohen, 2013: Variations of OH radical in an urban plume inferred from NO2 column measurements. *Geophysical Research Letters*, **40 (9)**, 1856–1860, https://doi.org/https://doi.org/10.1002/grl.50267, URL https://agupubs.onlinelibrary.wiley.com/doi/abs/10.1002/grl.50267, https://agupubs.onlinelibrary.wiley.com/doi/pdf/10.1002/grl.50267.

Valmassoi, A., and Coauthors, 2023: Current challenges and future directions in data assimilation and reanalysis. *Bulletin of the American Meteorological Society*, **104**, E756–E767, https://doi.org/10.1175/BAMS-D-21-0331.1.

Van Damme, M., L. Clarisse, S. Whitburn, J. Hadji-Lazaro, D. Hurtmans, C. Clerbaux, and P.-F. Coheur, 2018: Industrial and agricultural ammonia point sources exposed. *Nature*, **564**, 99–103, https://doi.org/10.1038/s41586-018-0747-1.

Van Damme, M., S. Whitburn, L. Clarisse, C. Clerbaux, D. Hurtmans, and P.-F. Coheur, 2017: Version 2 of the IASI NH_3 neural network retrieval algorithm: near-real-time and reanalysed datasets. *Atmospheric Measurement Techniques*, **10**, 4905–4914, https://doi.org/10.5194/amt-10-4905-2017.

van der A, R. J., A. T. J. de Laat, J. Ding, and H. J. Eskes, 2020: Connecting the dots: NOx emissions along a West Siberian natural gas pipeline. *npj Climate and Atmospheric Science*, **3**, 16, https://doi.org/10.1038/s41612-020-0119-z.

van der A, R. J., J. Ding, and H. Eskes, 2024: Monitoring European anthropogenic NOx emissions from space. *EGUsphere*, **2024**, 1–20, https://doi.org/10.5194/egusphere-2023-3099, URL https://egusphere.copernicus.org/preprints/2024/egusphere-2023-3099/.

van der Graaf, S., E. Dammers, A. Segers, R. Kranenburg, M. Schaap, M. W. Shephard, and J. W. Erisman, 2022: Data assimilation of CrIS NH_3 satellite observations for improving spatiotemporal NH_3 distributions in LOTOS-EUROS. *Atmospheric Chemistry and Physics*, **22**, 951–972, https://doi.org/10.5194/acp-22-951-2022.

Van Geffen, J., and Coauthors, 2022: Sentinel-5P TROPOMI NO_2 retrieval: impact of version v2.2 improvements and comparisons with OMI and ground-based data. *Atmospheric Measurement Techniques*, **15**, 2037–2060, https://doi.org/10.5194/amt-15-2037-2022.

Varon, D. J., D. J. Jacob, J. McKeever, D. Jervis, B. O. A. Durak, Y. Xia, and Y. Huang, 2018: Quantifying methane point sources from fine-scale satellite observations of atmospheric methane plumes. *Atmospheric Measurement Techniques*, **11 (10)**, 5673–5686, https://doi.org/10.5194/amt-11-5673-2018, URL https://amt.copernicus.org/articles/11/5673/2018/.

Veefkind, J., J. de Haan, E. Brinksma, M. Kroon, and P. Levelt, 2006: Total ozone from the ozone monitoring instrument (OMI) using the DOAS technique. *IEEE Transactions on Geoscience and Remote Sensing*, **44 (5)**, 1239–1244, https://doi.org/10.1109/TGRS.2006.871204.

Veefkind, J., and Coauthors, 2012: TROPOMI on the ESA Sentinel-5 Precursor: A GMES mission for global observations of the atmospheric composition for climate, air quality and ozone layer applications. *Remote Sensing of Environment*, **120**, 70–83, https://doi.org/10.1016/j.rse.2011.09.027.

Vu Van, A., and Coauthors, 2023: Near-real-time detection of unexpected atmospheric events using principal component analysis on the Infrared Atmospheric Sounding Interferometer (IASI) radiances. *Atmospheric Measurement Techniques*, **16**, 2107–2127, https://doi.org/10.5194/amt-16-2107-2023.

Wang, J. S., S. R. Kawa, G. J. Collatz, M. Sasakawa, L. V. Gatti, T. Machida, Y. Liu, and M. E. Manyin, 2018: A global synthesis inversion analysis of recent variability in CO_2 fluxes using GOSAT and in situ observations. *Atmospheric Chemistry and Physics*, **18**, 11 097–11 124, https://doi.org/10.5194/acp-18-11097-2018.

Wang, M., X. Chen, Z. Jiang, T.-L. He, D. Jones, J. Liu, and Y. Shen, 2024: Meteorological and anthropogenic drivers of surface ozone change in the north china plain in 2015–2021. *Science of The Total Environment*, **906**, 167 763, https://doi.org/https://doi.org/10.1016/j.scitotenv.2023.167763, URL https://www.sciencedirect.com/science/article/pii/S0048969723063908.

Wang, Y., G. P. Brasseur, and T. Wang, 2022: Segregation of atmospheric oxidants in turbulent urban environments. *Atmosphere*, **13**, 315, https://doi.org/10.3390/atmos13020315.

Wang, Y., J. Wang, X. Xu, D. K. Henze, Z. Qu, and K. Yang, 2020: Inverse modeling of SO_2 and NO_x emissions over China using multisensor satellite data – Part 1: Formulation and sensitivity analysis. *Atmospheric Chemistry and Physics*, **20**, 6631–6650, https://doi.org/10.5194/acp-20-6631-2020.

Wang, Y., and X. Wang, 2023: Simultaneous multiscale data assimilation using scale- and variable-dependent localization in envar for convection allowing analyses and forecasts: Methodology and experiments for a tornadic supercell. *Journal of Advances in Modeling Earth Systems*, **15**, https://doi.org/10.1029/2022MS003430.

Watine-Guiu, M., D. J. Varon, I. Irakulis-Loitxate, N. Balasus, and D. J. Jacob, 2023: Geostationary satellite observations of extreme and transient methane emissions from oil and gas infrastructure. *Proceedings of the National Academy of Sciences*, **120 (52)**, e2310797 120, https://doi.org/10.1073/pnas.2310797120, URL https://www.pnas.org/doi/abs/10.1073/pnas.2310797120, https://www.pnas.org/doi/pdf/10.1073/pnas.2310797120.

Wei, J., and Coauthors, 2020: Improved 1 km resolution $PM_{2.5}$ estimates across China using enhanced space–time extremely randomized trees. *Atmospheric Chemistry and Physics*, **20**, 3273–3289, https://doi.org/10.5194/acp-20-3273-2020.

Wells, K., and Coauthors, 2024: Long-term global measurements of methanol, ethene, ethyne, and HCN from the Cross-track Infrared Sounder. *EGUsphere*, **2024**, 1–40, https://doi.org/10.5194/egusphere-2024-1551, URL https://egusphere.copernicus.org/preprints/2024/egusphere-2024-1551/.

Wells, K. C., and Coauthors, 2020: Satellite isoprene retrievals constrain emissions and atmospheric oxidation. *Nature*, **585 (7824)**, 225–233, https://doi.org/10.1038/s41586-020-2664-3.

Wells, K. C., and Coauthors, 2022: Next-generation isoprene measurements from space: Detecting daily variability at high resolution. *Journal of Geophysical Research: Atmospheres*, **127 (5)**, https://doi.org/10.1029/2021jd036181.

West, J. J., and Coauthors, 2013: Co-benefits of mitigating global greenhouse gas emissions for future air quality and human health. *Nature Climate Change*, **3 (10)**, 885–889, https://doi.org/10.1038/nclimate2009, URL https://doi.org/10.1038/nclimate2009.

Whitburn, S., and Coauthors, 2016: A flexible and robust neural network IASI-NH3 retrieval algorithm. *Journal of Geophysical Research: Atmospheres*, **121 (11)**, 6581–6599, https://doi.org/10.1002/2016jd024828.

Wiedinmyer, C., R. J. Yokelson, and B. K. Gullett, 2014: Global emissions of trace gases, particulate matter, and hazardous air pollutants from open burning of domestic waste. *Environmental Science & Technology*, **48**, 9523–9530, https://doi.org/10.1021/es502250z.

Wright, C. J., and Coauthors, 2022: Surface-to-space atmospheric waves from hunga tonga–hunga ha'apai eruption. *Nature*, **609 (7928)**, 741–746, https://doi.org/10.1038/s41586-022-05012-5, URL https://doi.org/10.1038/s41586-022-05012-5.

Yang, D., J. Hakkarainen, Y. Liu, I. Ialongo, Z. Cai, and J. Tamminen, 2023a: Detection of Anthropogenic CO2 Emission Signatures with TanSat CO2 and with Copernicus Sentinel-5 Precursor (S5P) NO2 Measurements: First Results. *Advances in Atmospheric Sciences*, **40**, 1–5, https://doi.org/10.1007/s00376-022-2237-5.

Yang, J., Z. Zhang, C. Wei, F. Lu, and Q. Guo, 2017: Introducing the New Generation of Chinese Geostationary Weather Satellites, Fengyun-4. *Bulletin of the American Meteorological*

Society, **98 (8)**, 1637 – 1658, https://doi.org/10.1175/BAMS-D-16-0065.1, URL https://journals.ametsoc.org/view/journals/bams/98/8/bams-d-16-0065.1.xml.

Yang, L. H., and Coauthors, 2023b: Tropospheric NO_2 vertical profiles over South Korea and their relation to oxidant chemistry: implications for geostationary satellite retrievals and the observation of NO_2 diurnal variation from space. *Atmospheric Chemistry and Physics*, **23 (4)**, 2465–2481, https://doi.org/10.5194/acp-23-2465-2023, URL https://acp.copernicus.org/articles/23/2465/2023/.

Yumimoto, K., I. Uno, and S. Itahashi, 2014: Long-term inverse modeling of Chinese CO emission from satellite observations. *Environmental Pollution*, **195**, 308–318, https://doi.org/10.1016/j.envpol.2014.07.026.

Zeng, Z.-C., B. Franco, L. Clarisse, L. Lee, C. Qi, and F. Lu, 2024: Observing a Volatile Organic Compound from a Geostationary Infrared Sounder: HCOOH from FengYun-4B/GIIRS. https://doi.org/10.22541/essoar.171415918.82964609/v1, URL http://dx.doi.org/10.22541/essoar.171415918.82964609/v1.

Zeng, Z.-C., L. Lee, and C. Qi, 2023a: Diurnal carbon monoxide observed from a geostationary infrared hyperspectral sounder: first result from GIIRS on board FengYun-4B. *Atmospheric Measurement Techniques*, **16 (12)**, 3059–3083, https://doi.org/10.5194/amt-16-3059-2023, URL https://amt.copernicus.org/articles/16/3059/2023/.

Zeng, Z.-C., L. Lee, C. Qi, L. Clarisse, and M. Van Damme, 2023b: Optimal estimation retrieval of tropospheric ammonia from the Geostationary Interferometric Infrared Sounder on board FengYun-4B. *Atmospheric Measurement Techniques*, **16 (15)**, 3693–3713, https://doi.org/10.5194/amt-16-3693-2023, URL https://amt.copernicus.org/articles/16/3693/2023/.

Zhang, B., and Coauthors, 2023: Machine learning assesses drivers of PM2.5 air pollution trend in the Tibetan Plateau from 2015 to 2022. *Science of The Total Environment*, **878**, 163 189, https://doi.org/https://doi.org/10.1016/j.scitotenv.2023.163189, URL https://www.sciencedirect.com/science/article/pii/S0048969723018089.

Zhang, H., Z. Wei, B. H. Henderson, S. C. Anenberg, K. O'Dell, and S. Kondragunta, 2022: Nowcasting Applications of Geostationary Satellite Hourly Surface PM2.5 Data. *Weather and Forecasting*, **37**, 2313–2329, https://doi.org/10.1175/WAF-D-22-0114.1.

Zhao, C., and Y. Wang, 2009: Assimilated inversion of NO_x emissions over east Asia using OMI NO_2 column measurements. *Geophysical Research Letters*, **36**, https://doi.org/10.1029/2008GL037123.

Zheng, B., and Coauthors, 2018: Trends in China's anthropogenic emissions since 2010 as the consequence of clean air actions. *Atmospheric Chemistry and Physics*, **18 (19)**, 14 095–14 111, https://doi.org/10.5194/acp-18-14095-2018, URL https://acp.copernicus.org/articles/18/14095/2018/.

Zheng, B., and Coauthors, 2019: Global atmospheric carbon monoxide budget 2000–2017 inferred from multi-species atmospheric inversions. *Earth System Science Data*, **11 (3)**, 1411–1436, https://doi.org/10.5194/essd-11-1411-2019.

Zoogman, P., and Coauthors, 2017: Tropospheric emissions: Monitoring of pollution (TEMPO). *Journal of Quantitative Spectroscopy and Radiative Transfer*, **186**, 17–39, https://doi.org/10.1016/j.jqsrt.2016.05.008.

Zuo, X., and Coauthors, 2023: Observing Downwind Structures of Urban HCHO Plumes From Space: Implications to Non-Methane Volatile Organic Compound Emissions. *Geophysical Research Letters*, **50 (24)**, e2023GL106 062, https://doi.org/https://doi.org/10.1029/2023GL106062, URL https://agupubs.onlinelibrary.wiley.com/doi/abs/10.1029/2023GL106062, e2023GL106062 2023GL106062, https://agupubs.onlinelibrary.wiley.com/doi/pdf/10.1029/2023GL106062.